

Inherent gravitational instability of hot continental crust: Implications for doming and diapirism in granulite facies terrains

Taras V. Gerya*

Geological Institute, Swiss Federal Institute of Technology Zurich, CH 8092 Zurich, Switzerland, and Institute of Experimental Mineralogy, Russian Academy of Sciences, Chernogolovka, Moscow District 142432, Russia

Leonid L. Perchuk

Department of Petrology, Geological Faculty, Moscow State University, Vorobievsky Gory, Moscow 119899, Russia

Walter V. Maresch

Arne P. Willner

Institute of Geology, Mineralogy and Geophysics, Ruhr-University Bochum, 44780 Bochum, Germany

ABSTRACT

Modeling of in situ rock properties based on a Gibbs free energy minimization approach shows that regional metamorphism of granulite facies may critically enhance the decrease of crustal density with depth. This leads to a gravitational instability of hot continental crust, resulting in regional doming and diapirism. Two types of crustal models have been studied: (1) lithologically *homogeneous* crust and (2) *heterogeneous*, multilayered crust. Gravitational instability of relatively homogeneous continental crust sections is related to a vertical density contrast developed during prograde changes in mineral assemblages and the thermal expansion of minerals with increasing temperature. Gravitational instability of lithologically heterogeneous crust is related to an initial density contrast of dissimilar intercalated layers enhanced by high-temperature phase transformations. In addition, the thermal regime of heterogeneous crust strongly depends on the pattern of vertical interlayering: A strong positive correlation between temperature and the estimated degree of lithological gravitational instability is indicated. An interrelated combination of two-dimensional, numerical thermomechanical experiments and modeling of in situ physical properties of rocks is used to study the processes of gravitational redistribution within a doubly stacked, heterogeneously layered continental crust. It is shown that exponential lowering of viscosity with increasing temperature, in conjunction with prograde changes in metamorphic mineral assemblages during thermal relaxation after collisional thickening of the crust, provide positive feedback mechanisms leading to regional doming and diapirism that contribute to the exhumation of high-grade metamorphic rocks.

Keywords: granulite facies metamorphism, rock density modeling, high-grade terrains, collision, two-dimensional numerical experiments, gravitational redistribution.

*Taras.Gerya@erdw.ethz.ch

INTRODUCTION

Numerous structural, geochronological, and petrological studies have considered the tectono-metamorphic processes leading to the formation of granulite complexes within continental crust (see reviews by Harley, 1989; Thompson, 1990; Spear, 1993). In a review by Harley (1989) of about 90 granulite complexes, a remarkable diversity in granulite characteristics, particularly in the retrograde P - T paths, was emphasized. This diversity mirrors the variety of tectonic histories of granulites. Hence, no single universal tectonic model for the origin and exhumation of granulites can be advocated (Harley, 1989).

While tectonic models of formation of different granulite complexes are diverse, however, it is widely believed that the driving forces operating during their geodynamic histories are of an *external* nature with respect to the continental crust itself. For example, the most important geodynamic processes considered for the origin of granulites (see reviews by Harley, 1989; Thompson, 1990; Spear, 1993) are (1) tectonic thickening or thinning of the continental crust, (2) magmatic underplating (magmatic accretion), (3) delamination of cold mantle lithosphere, and (4) tectonic exhumation of crustal blocks associated with erosion.

In this respect, an important suggestion was made by Perchuk (1989), who emphasized the critical role of *internal* crustal buoyancy forces (Ramberg, 1981) as a factor in the exhumation of some Precambrian granulite terrains in hot continental crust characterized by extremely low dP/dT gradients. Because of the exponential decrease in the viscosity of rocks with increasing temperature (e.g., Turcotte and Schubert, 1982; Ranalli, 1995), high-grade granulite facies metamorphism could trigger processes of crustal doming and diapirism (Ramberg, 1981; Perchuk, 1989) in gravitationally unstable continental crust. The general validity of a gravitational instability model for the exhumation of granulites has been underlined by numerical geodynamic experiments (Perchuk et al., 1992), including the numerical modeling of different types of P - T paths (Gerya et al., 2000).

The following major possibilities for the formation of gravitationally unstable continental crust sections have been discussed in the literature:

1. *Magmatic processes:*

- the invasion of mafic magmas in the form of huge quantities of lava pouring out on the top of continental crust (e.g., plateau basalt) or injected as sills, dykes, and plutons within continental crust (Ramberg, 1981; Gerya et al., this volume, Chapter 8);
- the emplacement of mafic and ultramafic volcanic and plutonic rocks within greenstone belts situated in the upper portion of cratonic successions in granite-greenstone belts (e.g., Ramberg, 1981; Perchuk, 1989; Perchuk et al., 1992);
- the formation of thick volcano-sedimentary successions with medium-scale (0.1–4 km), rhythmic intercalation of rocks of different densities within the crust; although the individual low-density, gravitationally unstable layers are

thin, gravitational redistribution processes can lead to merging of several low density layers and result in the growth of large domes and diapirs (Perchuk et al., 1992); and

- crustal anatexis and granitization processes, granitoid intrusion, charnockitization, and melting related to high-grade metamorphism (e.g., Ramberg, 1981; Perchuk, 1989; Bittner and Schmeling, 1995).

2. *Tectonic processes:*

- selective thickening of the continental crust in orogenic belts (e.g., Ramberg, 1981); and
- regional stacking of continental crust during collision, creating a potentially unstable thickened crust in areas with initially stable crustal profiles (e.g., Gerya et al., 2002a).

3. *Metamorphic phase transformations:*

- the lowering of crustal density with depth, due mainly to prograde changes in mineral assemblages and the thermal expansion of minerals (Gerya et al., 2001).

The major purpose of this paper is to quantify the influence of changes in the vertical lithological and mineralogical structure of the continental crust on the degree of its gravitational instability and on the development of crustal doming and diapirism. Of particular interest are the processes expected to proceed in thickened continental crust during its thermal relaxation. As is well known, it is primarily collision that will lead to either homogeneous thickening or multiple stacking of initially stable crustal profiles (e.g., Ramberg, 1981; Turcotte and Schubert, 1982; England and Thompson, 1984; De Wit and Ashwal, 1997; Krohe, 1998; Le Pichon et al., 1997). Post-collisional processes of doming and diapirism can be due either to primary density contrasts in the stacked crust (Gerya et al., 2002a) or to inversions of rock densities caused by reequilibration leading to either partial melting at relatively high water fugacities (e.g., Bittner and Schmeling, 1995; Arnold et al., 2001) or to a granulite-facies overprint with the production of mineral assemblages of comparatively lower density (Gerya et al., 2001).

To quantify these interrelated tectono-metamorphic processes, we use a novel combination of a Gibbs free energy minimization approach (e.g., Karpov et al., 1976; de Capitani and Brown, 1987; Sobolev and Babeyko, 1994; Gerya et al., 2001) with thermomechanical numerical experiments.

MODELING OF IN SITU ROCK DENSITY

Methodology

We have used a Gibbs free energy minimization procedure to calculate equilibrium assemblages and compositions of minerals for a given pressure, temperature, and rock composition. The density was then calculated as the ratio of the sum of the molar masses to the sum of the molar volumes of the constituent minerals, where each mass and volume is weighted by the molar abundance of the mineral in the rock. We have employed the recently developed Gibbs free energy minimization code DEKAP (Gerya et al., 2001), which is based on a modified version of the

algorithm suggested by de Capitani and Brown (1987) for complex systems containing non-ideal solid solutions. Thermodynamic data for minerals and aqueous fluid were taken from the internally consistent database of Holland and Powell (1998), which is widely used in petrological studies of metamorphic rocks. Mixing models of solid solutions consistent with this database were taken from the literature (Holland and Powell, 1998; Holland et al., 1998; Powell and Holland, 1999; Dale et al., 2000). Two types of calculations were performed: (1) determination of petrogenetic grids and corresponding density maps with a resolution of 5 K and 100 bar for T and P , respectively, and (2) calculation of density profiles along geotherms with a resolution of 100 m (~ 30 bar). For crustal density profiles, equilibrium assemblages were calculated at temperatures ≥ 300 °C. At lower temperatures, the assemblages calculated for $T = 300$ °C were assumed to be present.

We considered six different types of metamorphic rocks as possible major lithologies for the crust as a whole (Table 1): granodioritic (UC), andesitic (AC), and gabbroic (LC) crust (McLennan, 1992), high-grade metapelite (MP) (Yardley, 1989), typical Precambrian granulite (KG) represented by the average composition of the Kanskii granulite complex, Yenisey Range, Eastern Siberia (Nozkhin and Turkina, 1993), and the average composition of Archean felsic granulites (FG) (Rudnick and Fountain, 1995). Molar abundances of minerals were calculated from bulk rock compositions (Table 1) using a system of mass-balance equations for 10 components: SiO_2 , TiO_2 , Al_2O_3 , MgO , Fe_2O_3 , FeO , CaO , Na_2O , K_2O , and H_2O . To avoid unrealistic mineral assemblages, cordierite, andalusite, and sillimanite had to be considered as unstable in clinopyroxene-normative rocks (UC, AC, LC, FG). For the same reason, calcic amphibole and clinopyroxene were considered unstable in Al-rich metapelites (MP). The system was considered to be open for H_2O (i.e., the

volatiles produced in dehydration reactions were assumed to be removed); therefore, although fluid phase saturation was ensured for all calculated equilibrium mineral assemblages, such fluids were not involved in density calculations. P - T -dependent volumes of phases, V , in equilibrium mineral assemblages were calculated via the Gibbs potential, G , using the thermodynamic relation $V = \partial G / \partial P$ and a numerical differentiation procedure.

The influence of partial melting on the gravitational instability of the crust has already been studied theoretically using numerical thermomechanical modeling (e.g., Bittner and Schmeling, 1995). In our study we have therefore concentrated on melt-absent conditions typical for many granulite facies terrains. In order to simulate these conditions, a lowered water activity was assumed at temperatures above 630 °C (cf., granite solidus in Fig. 1A), according to the following empirical equation (Gerya et al., 2001):

$$a_{\text{H}_2\text{O}} = 1.0 - [(T_{\text{K}} + 20 - t_1)/(t_2 - t_1)1.2]^{0.865}, \quad (1)$$

where

$$\begin{aligned} t_1 &= 877 + 160/(P_{\text{kbar}} + 0.348)^{0.75}, \\ t_2 &= 1262 + 9P_{\text{kbar}} \\ 0.1 &< a_{\text{H}_2\text{O}} < 1.0. \end{aligned}$$

Equation (1) was calibrated using data on the P - T parameters of the granite solidus calculated for different $a_{\text{H}_2\text{O}}$ (Johannes, 1985). This equation allows us to constrain the granite melting temperature at 20 K above the given temperature, T_{K} , for a given pressure, P_{kbar} and provides a transition to the conditions of granulite facies metamorphism characterized by a lowered water activity, $a_{\text{H}_2\text{O}}$ (Harley, 1989; Thompson, 1990; Spear, 1993).

Results of Density Calculations

Simplified petrogenetic grids and corresponding density maps obtained for the rocks studied (Table 1) are presented in Figures 1 and 2, and examples of calculated crustal density profiles along different geotherms are shown in Figure 3. Figures 1–2 show that, in the P - T plane, the density generally decreases toward lower pressures and higher temperatures for all types of rocks. For geotherms with low dP/dT slopes, high densities are characteristic for greenschist and, in part, low-grade amphibolite facies rocks, and low densities are obtained for high-grade amphibolite and granulite facies rocks of low to moderate pressure. The moderate slope of the high temperature geotherms C–G in Figure 1 is in significant contrast to the steep slope of the contours of constant density, resulting in a general decrease in density with increasing depth along these geotherms (Fig. 3). Sharp density changes are characteristic for dehydration reactions and produce step-like changes in density with depth (Fig. 3). For rocks of metapelite (MP) and typical acid granulite (KG) composition, a marked density minimum is observed between 15 and 25 km in depth. The decrease in density with increase in

TABLE 1. ROCK COMPOSITIONS* USED FOR DENSITY CALCULATIONS

	UC†	LC†	AC†	KG†	MP†	FG†
SiO_2	66.12	54.48	57.94	65.81	65.30	71.34
TiO_2	0.50	1.00	0.80	0.81	0.81	0.40
Al_2O_3	15.24	16.14	17.94	15.24	17.84	14.57
Fe_2O_3 §	1.03	2.42	1.70	1.73	1.61	0.71
FeO	3.39	7.97	5.62	5.71	5.33	2.35
MgO	2.21	6.32	3.50	2.73	2.38	1.11
CaO	4.21	8.52	7.49	2.73	1.27	2.83
Na_2O	3.91	2.81	3.50	2.12	2.02	3.85
K_2O	3.38	0.34	1.50	3.13	3.44	2.83

*in weight %, sums of oxides normalized to 100%.

†abbreviations used: UC, LC, and AC—upper granodioritic, lower gabbroic, and andesitic crust, respectively (McLennan, 1992); MP—typical high-grade metapelite composition (Yardley, 1989); KG—average composition of granulites of the Kanskii complex (Yenisey Range, Eastern Siberia) (Nozkhin and Turkina, 1993); FG—average composition of Precambrian felsic granulites (Rudnick and Fountain, 1995).

§ Fe^{3+} is taken as 25 atomic percent of total Fe.

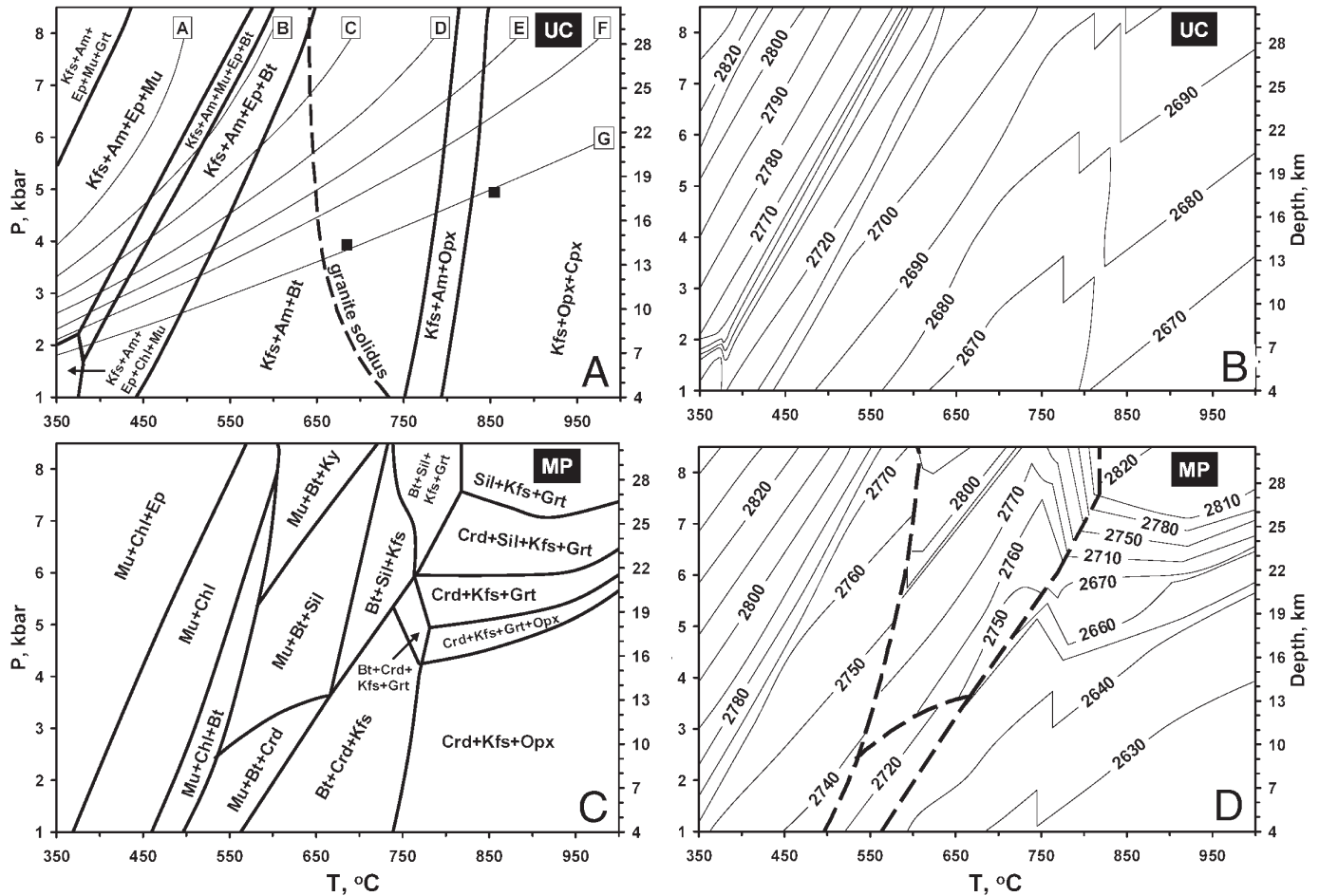


Figure 1. Petrogenetic grids (A, C) and density (kg/m^3) maps (B, D) calculated for crust of granodioritic composition (A, B) (see UC in Table 1) and for typical high-grade metapelite (C, D) (see MP in Table 1). Quartz, plagioclase, and Fe-Ti oxides are present in all mineral assemblages. Heavy dashed line in A corresponds to H_2O -saturated granite solidus (Johannes, 1985). Heavy dashed lines in D indicate important changes in mineral assemblages. Thin lines labeled A–G correspond to different crustal geotherms (Gerya et al., 2001). Black solid rectangles in A show peak metamorphic conditions estimated for granulite (Waters, 1989) and amphibolite (Willner, 1995) zones in the Namaqualand granulite terrain. Abbreviations of mineral names are after Kretz (1983).

metamorphic grade is mainly related to reactions producing anorthite-rich plagioclase (instead of epidote), sillimanite (instead of kyanite), and cordierite. This causes the significant ($40\text{--}150 \text{ kg/m}^3$) decrease in crustal density with depth for high-temperature geotherms characterized by low dP/dT gradients (Fig. 3). This decrease represents the combined influence of both the P - V - T properties of individual minerals as well as the metamorphic reactions leading to changes in mineral assemblages.

DEGREE OF GRAVITATIONAL INSTABILITY OF THE CRUST

Homogeneous Continental Crust Sections

The results of density calculations suggest a considerable ($50\text{--}150 \text{ kg/m}^3$) decrease of rock densities with depth (Fig. 3)

for hot continental crust of relatively homogeneous lithological composition and vertical metamorphic zoning, leading to low- to medium-pressure granulite facies metamorphism. This decrease should be especially characteristic for crust of felsic to intermediate composition (Fig. 3A, B). Figure 3 shows that a zone with a density minimum could appear in the crust when the temperature at its base exceeds $600\text{--}700 \text{ }^\circ\text{C}$. For temperatures exceeding $800 \text{ }^\circ\text{C}$, which is typical for medium- to low-pressure granulite facies conditions (e.g., Harley, 1989), the thickness of the low-density layer could reach $5\text{--}15 \text{ km}$, providing a high degree of internal gravitational instability for the crust.

The degree of instability can be quantified in terms of the maximum internal gravitational energy that can be released by gravitational redistribution. For any given density profile, this value can be estimated by comparison to a gravitationally stable “ordered” profile, in which the volume ratios of rocks with

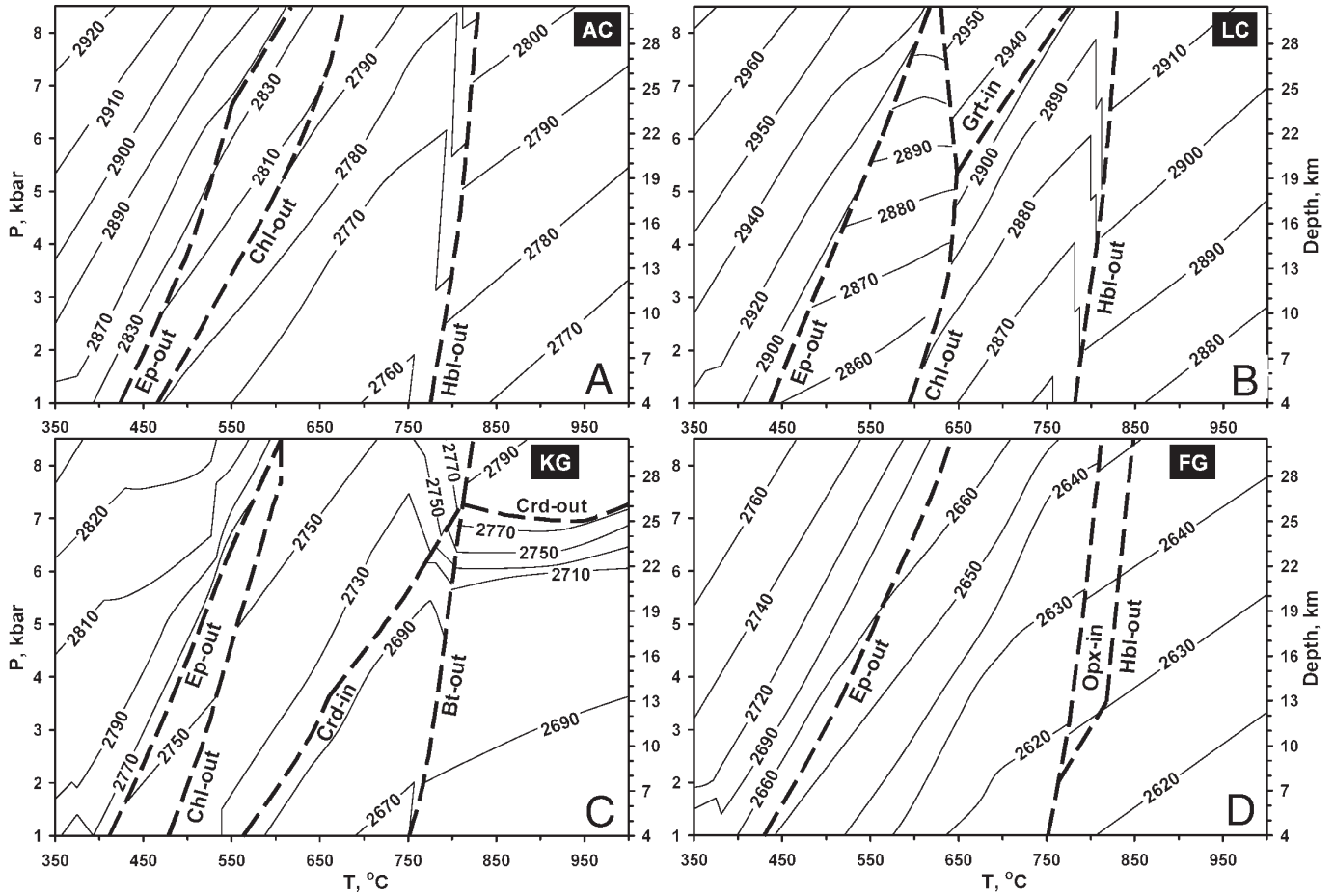


Figure 2. Density (kg/m^3) maps calculated for crust of andesitic (A) and gabbroic (B) composition (see AC and LC in Table 1), as well as the average compositions of the Kanskiy granulite complex (C) and Precambrian felsic granulites (D) (see KG and FG in Table 1). Heavy dashed lines indicate important changes in mineral assemblages.

various densities are equivalent but the density of crust does not decrease with depth. The following equation can then be used to calculate the maximum internal gravitational energy of the crust (Gerya et al., 2001):

$$U = g/h \int_{z=a}^h [\rho(z) - \rho_o(z)] (h - z) dz, \quad (2)$$

where U is the gravitational energy, J/m^3 , h is thickness of the crust, $\rho(z)$ and $\rho_o(z)$ are calculated and theoretical “ordered” density profiles with depth z , respectively, $g = 9.81 \text{ m}\cdot\text{s}^{-2}$ is the gravitational acceleration, a is the depth for $T = 400 \text{ }^\circ\text{C}$ (~lower limit of greenschist facies; Yardley, 1989). To avoid an overestimation of gravitational energy caused by the possible presence of non-metamorphosed or only partially metamorphosed rocks in the upper portion of the crust at temperatures $< 400 \text{ }^\circ\text{C}$, “ordering” of calculated density profiles was only considered in the a – h depth interval.

Figure 4 shows the gravitational energy of homogeneous crust as a function of temperature at its base. For most of the

studied crustal compositions, the degree of gravitational instability increases strongly within the temperature interval 600 – $800 \text{ }^\circ\text{C}$, which corresponds to high-grade amphibolite and granulite facies conditions. For crust of pelitic composition, this increase is shifted to higher temperatures of 800 – $1000 \text{ }^\circ\text{C}$ due to the stability of low-density, cordierite-bearing assemblages (Fig. 1C, D).

Heterogeneously Layered Continental Crust Sections

Using one-dimensional thermal modeling for multilayered (heterogeneous) continental crust, Gerya et al. (2002a) have shown that both the degree of gravitational instability and the thermal regime of this crust strongly depend on its vertical lithological structure. Figure 5 demonstrates the thermal effects of different patterns of vertical structuring of a granodioritic/gabbroic or granodioritic/dioritic crust while retaining a 1:1 volume ratio between the two respective bulk-compositional layer types (i.e., a constant bulk radiogenic heat supply within the crust) and a constant total crustal thickness of 50 km . The tested models

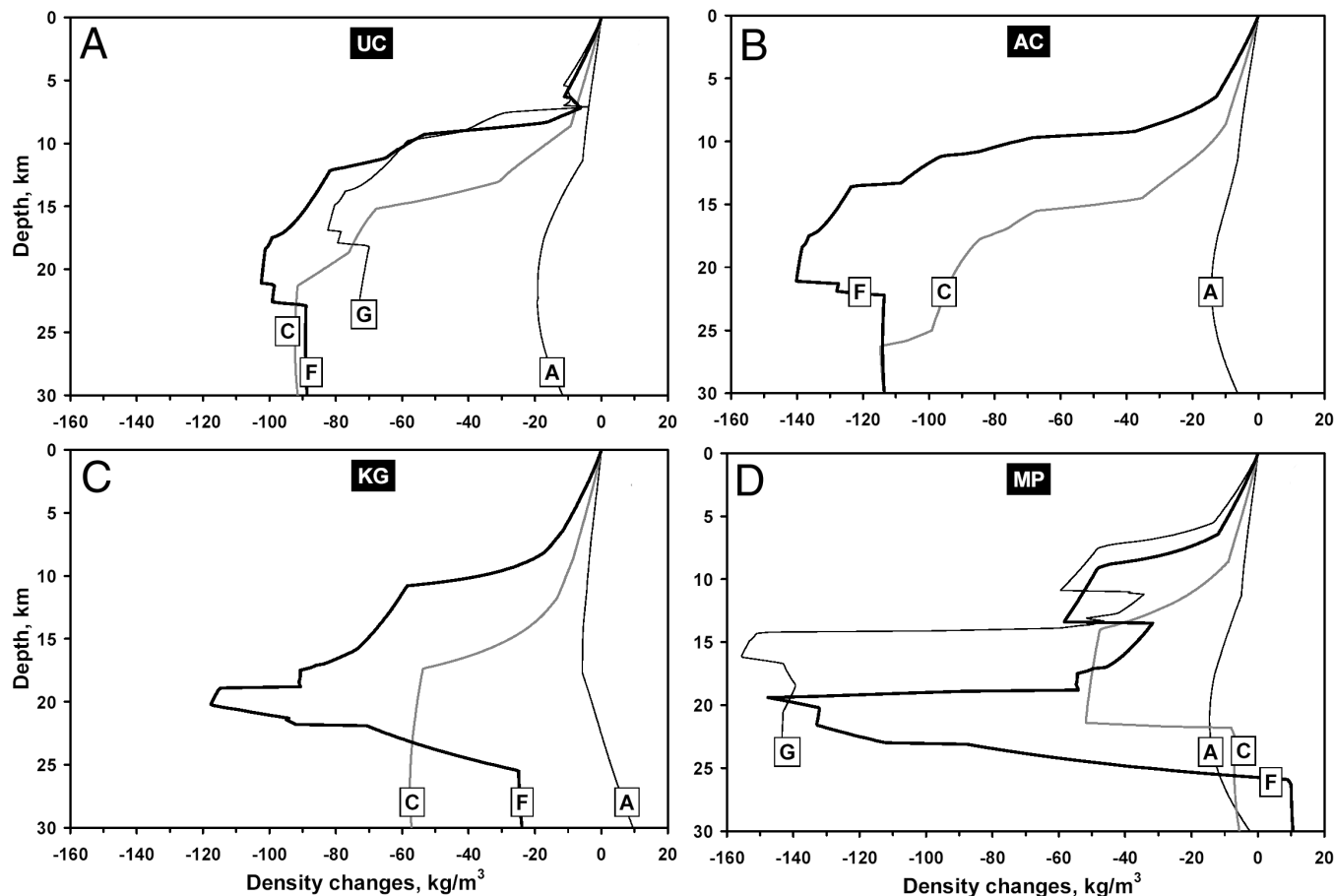


Figure 3. Typical examples of density profiles calculated along the geotherms shown in Figure 1A. UC—upper granodioritic crust; AC—andesitic crust; KG—granulites from the Kanskii complex; MP—metapelites.

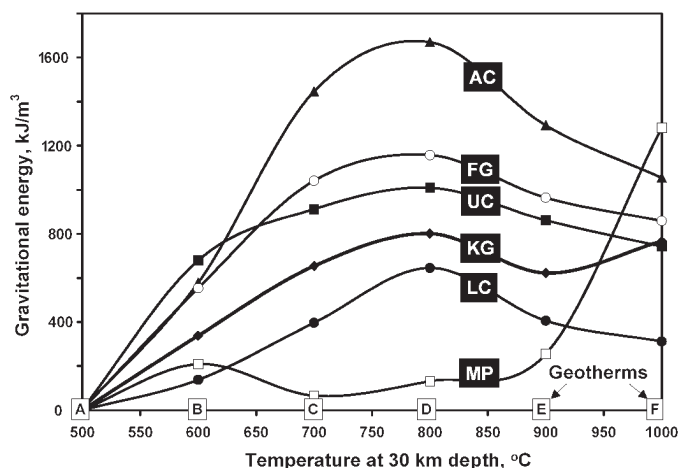


Figure 4. Gravitational energy of the homogeneous continental crust sections of various bulk compositions (Table 1) as a function of geothermal gradient. A–F correspond to A–F in Figure 1A. AC—andesitic crust; FG—felsic granulites; UC—upper granodioritic crust; KG—granulites from the Kanskii complex; LC—lower gabbroic crust; MP—metapelites.

illustrate an idealized progressive scheme and do not need to be directly related in detail to an actual, specific process of crustal formation. The models are applicable to any type of geodynamic process leading to specific contrasts and distribution patterns in density (cf. Introduction). The structural models 1–7 for the crust in Figure 5 represent a continuous increase of the degree of gravitational instability of the crust from a completely stable (model 1 in Fig. 5) to the most unstable (model 7 in Fig. 5) geometry. The degree of this lithological gravitational instability correlates positively with temperature along the calculated steady-state geotherm (for details of the calculations, see Gerya et al., 2002a): The more unstable the crust, the higher the temperature. The calculated shifts in steady-state geotherms caused by such variations in the internal geometry of the crust as a function of the distribution of the radiogenic heat supply are considerable. In the case of model 7, the temperature is about 300 °C higher at a depth of 30 km than that calculated with model 1 (Fig. 5A, B).

Figure 5C quantifies the correlation between the lithological structure and temperature in terms of maximum internal gravitational energy. For any given density profile, this energy can be estimated by comparison with a gravitationally stable “ordered”

profile (model 1 in Fig. 5) according to Equation 2. Figure 5C shows a strong positive correlation between the gravitational energy (i.e., degree of gravitational instability) of the crust, U , and temperatures at 30 km crustal level. Thus, the intercalation

of rocks with different densities and rates of radiogenic heat production leads to a strong correlation between gravitational and thermal structures. This correlation documents the net shift of the less dense, higher-heat-generating units toward greater depths and reflects the general negative correlation for rocks between radiogenic heat production on the one hand and density on the other.

Steady-state geotherms calculated for gravitationally unstable crust (Fig. 5A, B) will reflect the corresponding crustal thermal structure toward which the thickened crust will evolve after the geodynamic event and during the late-orogenic, non-steady stage. Figure 6 shows the results of one-dimensional combined modeling of the late-orogenic evolution of the thermal (Fig 6A), viscosity (Fig. 6B), and density (Fig. 6C) profiles within a double-stacked continental crust composed of rocks of granodioritic and dioritic compositions (for details of the calculations, see Gerya et al., 2002a). Figure 6 suggests that prograde metamorphic reactions (e.g., Fig. 1A) and increase of temperature in the lower crust (Fig. 6A) toward high grade amphibolite and granulite facies conditions result in significant enhancing of lithological density contrast and strong lowering of viscosity of the buried crust. This creates very favorable conditions for development of convective and Rayleigh-Taylor instabilities in hot heterogeneous stacked crust (Gerya et al., 2002a).

TWO-DIMENSIONAL NUMERICAL MODELING OF LATE OROGENIC DOMING AND DIAPIRISM IN STACKED CONTINENTAL CRUST

Initial and Boundary Conditions

Crustal/lithospheric thermal-chemical instability has been extensively studied with analytical and numerical methods as well as analogue modeling for various rheological and density structures (e.g., Ramberg, 1981; Weinberg and Schmeling, 1992; Bittner and Schmeling, 1995; Molnar et al., 1998; Houseman and Molnar, 1997; Jull and Kelemen, 2001; Conrad and Molnar, 1997, 1999). These studies show that the rheology of rocks is a major factor controlling the dynamics and time scales of thermal-chemical convection in gravitationally unstable structures (Molnar et al., 1998; Houseman and Molnar, 1997; Jull and Kelemen, 2001; Conrad and Molnar, 1997, 1999). According to the analytical estimates for two-layered crust with a 100–200 kg/m³ density contrast, time-scales of 10–100 m.y. are indicated for differential movement of rock masses on a kilometer scale when the effective viscosity of upper crustal rocks is lowered to $n \times 10^{21}$ Pa s (Gerya et al., 2001, 2002a).

Arnold et al. (2001) recently studied the late-orogenic evolution of a double-stacked crust underplated by hot asthenospheric mantle with two-dimensional thermomechanical numerical modeling experiments. The results show that, in the absence of erosion and external tectonic forces, partial melting and ductile rebound of the lower crust should be the dominant processes. Although buoyancy forces are present in the partially molten

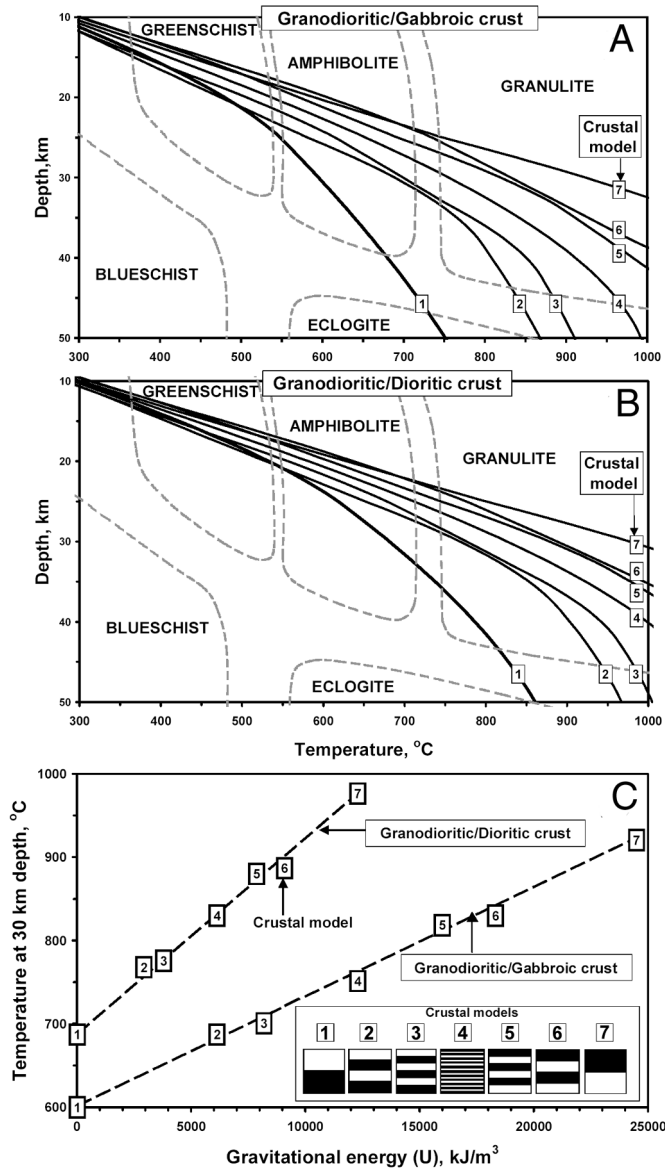


Figure 5. Steady-state geotherms (A, B) and gravitational energy (C) of heterogeneously layered continental crust models. Geotherms in A and B are calculated (Gerya et al., 2002a) for various types of restructured granodioritic/gabbroic (A) or granodioritic/dioritic (B) crust, retaining a 1:1 volume ratio between the two respective bulk-compositional layer types (i.e., a constant bulk radiogenic heat supply within the crust) and a constant total crustal thickness of 50 km. All other standard parameters are as in Table 2. Gravitational energy, U , of the crust (C) is calculated according to Equation (2) using the standard density ρ_0 (Table 2) of granodioritic (white) and gabbroic or dioritic (black) layers. A simplified facies scheme from Yardley (1989) is shown for orientation.

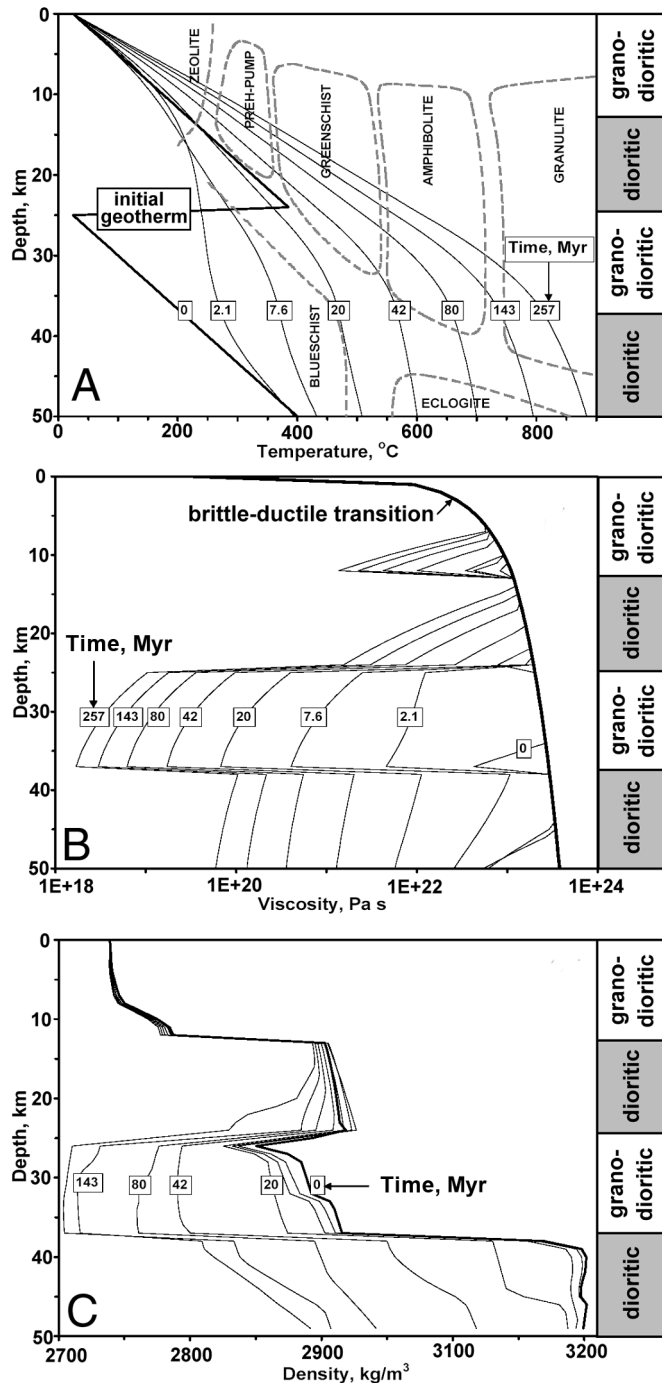


Figure 6. Results of one-dimensional modeling (Gerya et al., 2002a) of the evolution of the vertical temperature (A), viscosity (B), and density (C) profiles for a double-stacked crust composed of granodioritic and dioritic rocks (model 2 in Fig. 5C). A simplified facies scheme from Yardley (1989) in A is shown for orientation. The viscosity in B is calculated at a strain rate of 10^{-15} s^{-1} from experimentally determined rheological parameters given in Ranalli (1995); brittle-ductile transition (thick line) is calculated as “Mohr-Coulomb viscosity” (Equation 9) at a strain rate of 10^{-15} s^{-1} . Changes in crustal density in C are related to metamorphic phase transformations (Figs. 1 and 2).

lower crust, the viscosity of the overburden is too high to allow diapiric ascent (Arnold et al., 2001). On the other hand, the two-dimensional numerical model of Arnold et al. (2001) does not account for the effects of metamorphic phase transformations enhancing density contrast (e.g., Gerya et al., 2002a), nor does it account for the influence of erosion and sedimentation processes (Ellis et al., 2001). These factors may significantly change the dynamics of doming and diapirism within stacked continental crust.

Figure 7 depicts the initial geometry and thermal structure of double-stacked crust underlain by a lithospheric mantle typical for some collisional orogens (e.g., England and Thompson, 1984; Le Pichon et al., 1997). Figure 7 also shows the boundary conditions used in our model. To ensure a smooth continuity of the evolving material flow and a non-steady temperature field across the lower boundary of the truncated regional model, we have used a boundary condition involving the absence of a horizontal pressure gradient ($\partial P/\partial x = 0$) and the infinity-like condition for the temperature field (variable vertical Lagrangian heat flux corresponding to the condition $\partial^2 T/\partial z^2 = 0$; Turcotte and Schubert, 1973; Gerya et al., 2002b).

The upper surface is calculated dynamically at each time step as a free surface (e.g., Poliakov and Podladchikov, 1992; Gurnis et al., 1996). We have used an approximate scheme to account for the changes in topography by adding a layer with a lower viscosity (10^{16} Pa s) and higher heat conductivity ($20 \text{ W} \cdot \text{m}^{-1} \cdot \text{K}^{-1}$) with initial thickness of 10 km to the top of the continental crust. The effective viscosity contrast between this weak layer and the stronger upper crust in our experiments varied from 10^4 to 10^6 . As follows from analytical estimates for a two-layered model (Ramberg, 1981), the dynamics of topography of the layer interface stabilizes at viscosity contrasts $>10^3$, thus closely approximating a free surface condition for the stronger layer. The density of the weak layer is taken to be 1 kg/m^3 (air) at $z < 10 \text{ km}$ and 1000 kg/m^3 (seawater) at $z > 10 \text{ km}$, where z is the vertical distance from the top of the model. The interface between this layer and the top of the continental crust is considered to be the erosion/sedimentation surface, which evolves according to the following transport equation

$$\partial z_{\text{es}}/\partial t = v_z - v_x \partial z_{\text{es}}/\partial x - v_s + v_e, \quad (3)$$

where z_{es} is the vertical distance of the erosion/sedimentation surface from the top of the model as a function of the horizontal distance, x ; v_z and v_x are the vertical and horizontal components of the material velocity vector at the erosion/sedimentation surface, respectively; and v_s and v_e are, respectively, sedimentation and erosion rates corresponding to the relation

$$\begin{aligned} v_s &= 0 \text{ mm/a}, v_e = 0.1 \text{ mm/a} \text{ when } z < 10 \text{ km}, \\ v_s &= 0.1 \text{ mm/a}, v_e = 0 \text{ mm/a} \text{ when } z > 10 \text{ km}. \end{aligned}$$

At each time step, Equation (3) is solved numerically to calculate the corresponding vertical displacement of the erosion/

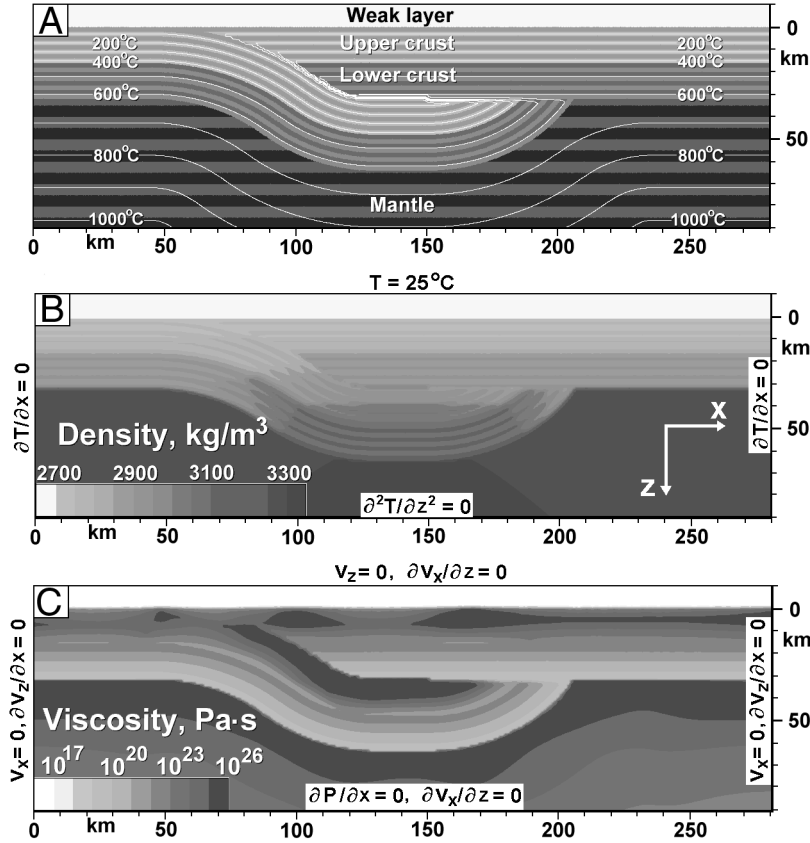


Figure 7. Design, initial, and boundary conditions of two-dimensional numerical experiments. The grid configuration is 281×101 ; regularly spaced points and 700,000 markers are employed. A. Initial lithological structure of the model consisting of 4 major rock types: sedimentary rocks (not yet formed, see Figs. 8 and 11); upper (granodioritic) crust; lower (either dioritic or gabbroic) crust, and lithospheric (ultramafic) mantle. Medium scale (~ 2 km) layering with constant (2%, ~ 50 kg/m³) density contrast in the continental crust is used to study multi-wavelength doming and diapirism phenomena (e.g., Weinberg and Schmeling, 1992), which accelerate regional gravitational redistribution (Perchuk et al., 1992). Non-compositional layering in the homogeneous mantle is used to show material displacement. B. Initial density structure of the model and thermal boundary conditions. C. Initial viscosity structure of the model and mechanical boundary conditions; the waviness in viscosity in the upper crust is related to the non-uniform stress distribution within the stacked crust. A color version of this figure is on the CD-ROM accompanying this volume.

sedimentation surface. There is a slight dynamic feedback from the topographical variations to the displacement of underlying rocks due to changes in the dynamic horizontal pressure gradients (e.g., Poliakov et al., 1993; Ellis et al., 2001).

In our numerical experiments, we have studied two types of initial crustal layering: (1) intercalation of rocks of granodioritic (upper crust) and gabbroic (lower crust) bulk composition, and (2) intercalation of rocks of granodioritic (upper crust) and dioritic (lower crust) bulk composition (Le Pichon et al., 1997; Gerya et al., 2002a). Medium scale (~ 2 km) layering with a constant (2%, ~ 50 kg/m³) density contrast is used to study multi-wavelength doming and diapirism phenomena (e.g., Weinberg and Schmeling, 1992), which accelerate regional gravitational redistribution (Perchuk et al., 1992). All physical properties of sedimentary rocks (Table 2) generated in the proximity of Earth's surface have been taken to be the same as for the granodioritic crust.

Mathematical Modeling and Numerical Implementation

We have considered two-dimensional creep flow, wherein both thermal and chemical buoyant forces are included along with heating from phase transformations, adiabatic compression, and viscous dissipation in the temperature equation. We employ the primitive variables of velocity, \underline{v} , and pressure, P , in the

momentum equation. To simplify modeling, we used the incompressible form of the continuity equation, which does not account for the volume changes during phase transformations

$$\partial v_x / \partial x + \partial v_z / \partial z = 0. \quad (4)$$

The two-dimensional Stokes equations with both thermal and chemical buoyancies take the form:

$$\partial \sigma_{xx} / \partial x + \partial \sigma_{xz} / \partial z = \partial P / \partial x, \quad (5)$$

$$\partial \sigma_{zz} / \partial z + \partial \sigma_{xz} / \partial x = \partial P / \partial z - g \rho(P, T, C, M). \quad (6)$$

The density $\rho(P, T, C, M)$ in the vertical component of the momentum equation depends explicitly on the pressure, P , temperature, T , the chemical composition, C , and the mineralogical composition, M .

We also employ realistic rheological constitutive relationships between the stress and strain-rate, whose coefficient, η , represents the effective viscosity $\eta(P, T, C, \dot{\epsilon})$, which depends on the chemical composition, temperature, pressure, and strain-rate $\dot{\epsilon}$

$$\begin{aligned} \sigma_{xx} &= 2\eta \dot{\epsilon}_{xx}, \\ \sigma_{xz} &= 2\eta \dot{\epsilon}_{xz}, \\ \sigma_{zz} &= 2\eta \dot{\epsilon}_{zz}, \\ \dot{\epsilon}_{xx} &= \partial v_x / \partial x, \end{aligned}$$

TABLE 2. THE SET OF STANDARD MATERIAL PROPERTIES* ASSUMED FOR CALCULATIONS

Rock type	Cp J/(K kg)	ρ_0 kg/m ³	α 10 ⁻⁵ /K	β 10 ⁻⁵ /MPa	k W/(m K)	Flow law	H_r 10 ⁻⁶ W/m ³
sedimentary	1000	2800	3	1	$0.64 + \frac{807}{T + 77}$	wet quartzite	2.0
granodioritic	1000	2800	3	1	$0.64 + \frac{807}{T + 77}$	wet quartzite	2.0
dioritic	1000	2900	3	1	$0.91 + \frac{641}{T + 77}$ †	quartz diorite	0.5
gabbroic	1000	3000	3	1	$1.18 + \frac{474}{T + 77}$	plagioclase (An ₇₅)	0.25
ultramafic	1000	3300	3	1	$0.73 + \frac{1293}{T + 77}$	dry olivine	0.022

*Standard material properties are taken from Turcotte and Schubert (1982), Ranalli (1995), Le Pichon et al., (1997); England and Thompson (1984); Clauser and Huenges (1995); the effective in situ material properties (Cp, ρ and α) of sedimentary, granodioritic, dioritic, and gabbroic rocks were calculated using a Gibbs energy minimization method (see text for details of calculations). Cp— isobaric heat capacity; k—thermal conductivity; ρ —density; α —thermal expansion coefficient; β —compressibility.

†thermal conductivity of dioritic rocks is taken as the average for granodioritic and gabbroic rocks

$$\begin{aligned}\dot{\epsilon}_{xz} &= \frac{1}{2}(\partial v_x / \partial z + \partial v_z / \partial x), \\ \dot{\epsilon}_{zz} &= \partial v_z / \partial z.\end{aligned}$$

The temperature equation takes the form

$$\begin{aligned}\rho Cp(\partial T / \partial t + v_x \partial T / \partial x + v_z \partial T / \partial z) \\ = \partial q_x / \partial x + \partial q_z / \partial z + H_r + H_a + H_s, \quad (7) \\ q_x = k(T) \times (\partial T / \partial x), \\ q_z = k(T) \times (\partial T / \partial z), \\ H_r = \text{constant}, \\ H_a = T\alpha[v_x(\partial P / \partial x) + v_z(\partial P / \partial z)] \approx T\alpha\rho v_z g, \\ H_s = \sigma_{xx} \dot{\epsilon}_{xx} + \sigma_{zz} \dot{\epsilon}_{zz} + 2\sigma_{xz} \dot{\epsilon}_{xz}.\end{aligned}$$

The notations used in Equations 4–7 are x and z , respectively, for the horizontal and vertical coordinates (Fig. 7B), in m; v_x and v_z for the components of velocity vector, \underline{v} , in $\text{m} \cdot \text{s}^{-1}$; t for time in s; σ_{xx} , σ_{zz} , and σ_{xz} for the components of the viscous deviatoric stress tensor in Pa; $\dot{\epsilon}_{xx}$, $\dot{\epsilon}_{zz}$, and $\dot{\epsilon}_{xz}$ for the components of the strain-rate tensor in s^{-1} ; P for the pressure in Pa; T for the temperature in K; q_x and q_z for the horizontal and vertical heat fluxes in $\text{W} \cdot \text{m}^{-2}$; η for the effective viscosity in $\text{Pa} \cdot \text{s}$; ρ for the density in $\text{kg} \cdot \text{m}^{-3}$; $g = 9.81 \text{ m} \cdot \text{s}^{-2}$ is the gravitational acceleration; $k(T)$ is the thermal conductivity $\text{W} \cdot \text{m}^{-1} \cdot \text{K}^{-1}$, which depends on the chemical composition and temperature (Table 2) according to Clauser and Huenges (1995); α is the effective coefficient of thermal expansion accounting for the effects of phase transformations in K^{-1} ; Cp is the effective isobaric heat capacity accounting for the effects of phase transformations in $\text{J} \cdot \text{kg}^{-1} \cdot \text{K}^{-1}$; and H_r , H_a , and H_s denote radioactive, effective adiabatic, and shear heat production in $\text{W} \cdot \text{m}^{-3}$, respectively.

We have employed the recently developed thermomechanical two-dimensional code I2 (Gerya et al., 2000) based on finite differences with a marker technique that allows for the accurate conservative solution of the governing equations on a rectangu-

lar half-staggered Eulerian grid for multiphase viscous flow. A detailed description of the numerical method and algorithmic tests are provided in Gerya et al. (2000).

Accounting for the Effects of Metamorphic Reactions

We used a novel algorithm (Gerya et al., 2002a) in order to model changes in the physical properties of crustal rocks (Table 1) related to metamorphic phase transformations (Figs. 1 and 2). Enthalpy and density have been tabulated using the Gibbs free energy minimization code DEKAP (Gerya et al., 2001) for $T = 0$ – 1000 °C (at 10 °C intervals) and $P = 1$ – $25,000$ bar (at intervals of 200 bar) for rocks of granodioritic (see UC in Table 1 and Fig. 1A, B), dioritic (see AC in Table 1 and Fig. 2A), and gabbroic (see LC in Table 1 and Fig. 2B) composition. For simplicity, it was assumed that complete reequilibration of a mineral assemblage is reached at a temperature above 400 °C. At lower temperatures, the enthalpy and the density were tabulated for the assemblage stable at $T = 400$ °C and the given pressure (with 1 kbar as a lower pressure limit). The effective in situ thermomechanical properties of the rocks (density, isobaric heat capacity, and thermal expansion) that account for the thermal effects of phase transformations were interpolated numerically during thermomechanical experiments via tabulated enthalpy (H) and density (ρ), according to the following standard thermodynamic relations:

$$\begin{aligned}Cp &= (\partial H / \partial T)_{P, \\ \alpha &= \rho T^{-1}[\rho^{-1} - (\partial H / \partial P)_{T,}].\end{aligned}$$

We also used a time-step limitation to ensure <10 °C changes in temperature for each calculation step.

We have not considered phase transformations for the mantle rock, and therefore used a constant heat capacity of 1000

J/(kg K) (Table 2). The density of the mantle rock was calculated according to the following equation:

$$\rho_{P,T} = \rho_0 [1 - \alpha(T - T_0)] \times [1 + \beta(P - P_0)], \quad (8)$$

where ρ_0 is the density at the standard pressure $P_0 = 0.1$ MPa and temperature $T_0 = 298$ K; α and β are, respectively, the thermal expansion and compressibility coefficients, which are taken to be constant (Table 2).

The Rheological Model

Following Schott and Schmelung (1998), we combined ductile creep rheology for rocks with a quasi-brittle rheology to yield an effective rheology. For this purpose, the Mohr-Coulomb law (Brace and Kohlstedt, 1980; Ranalli, 1995) was simplified to the yield stress, σ_{yield} , criterion and implemented by a ‘‘Mohr-Coulomb-viscosity,’’ η_{MC} , as follows:

$$\eta_{\text{MC}} = \frac{\sigma_{\text{yield}}}{(4\dot{\epsilon}_{\text{II}})^{1/2}}, \quad (9)$$

$$\sigma_{\text{yield}} = (M_1 P_{\text{lith}} + M_2)(1 - \lambda),$$

where $\dot{\epsilon}_{\text{II}} = \frac{1}{2}\dot{\epsilon}_{ij}$, $\dot{\epsilon}_{ij}$ is the second invariant of the strain-rate tensor, with dimension s^{-2} ; $\lambda = P_{\text{fluid}}/P_{\text{lith}}$ is the pore fluid pressure coefficient (i.e. the ratio between pore fluid pressure, P_{fluid} , and lithostatic pressure, P_{lith}); M_1 and M_2 in MPa are empirical constants ($M_1 = 0.85$, $M_2 = 0$ MPa when $\sigma_{\text{yield}} < 200$ MPa and $M_1 = 0.6$, $M_2 = 60$ MPa when $\sigma_{\text{yield}} > 200$ MPa [Brace and Kohlstedt, 1980]). The total effective viscosity, η , is then defined by the following criterion:

$$\eta = \eta_{\text{creep}} \text{ when } 2(\dot{\epsilon}_{\text{II}})^{1/2} \eta_{\text{creep}} < \sigma_{\text{yield}}, \quad (10a)$$

$$\eta = \eta_{\text{MC}} \text{ when } 2(\dot{\epsilon}_{\text{II}})^{1/2} \eta_{\text{creep}} > \sigma_{\text{yield}}. \quad (10b)$$

where η_{creep} is the creep viscosity, Pa s. The creep viscosity, which depends on the stress and temperature, is defined in terms of deformation invariants by (Ranalli, 1995):

$$\eta_{\text{creep}} = (\dot{\epsilon}_{\text{II}})^{(1-n)/2n} F (A_D)^{-1/n} \exp(E/nRT), \quad (11)$$

where F is a dimensionless coefficient depending on the type of experiments on which the flow law is based (e.g., $F = 2^{(1-n)/n}/3^{(1+n)/2n}$ for triaxial compression and $F = 2^{(1-2n)/n}$ for simple shear).

To represent the ductile rheology of different rocks, we used flow laws for dislocation creep of experimentally studied geomaterials (Table 2). Flow law parameters for Equation (10) determined for these materials are taken from the compilation of Ranalli (1995):

- gabbroic crust—flow law of plagioclase with composition An_{75} , with $E = 238$ kJ · mol⁻¹, $n = 3.2$, and $\log A_D = -3.5$ (A_D given in MPa⁻ⁿ · s⁻¹);
- dioritic crust—flow law of quartz diorite, with $E = 219$ kJ · mol⁻¹, $n = 2.4$, and $\log A_D = -2.9$;

- granodioritic crust and sedimentary rocks—flow law of wet quartzite, with $E = 154$ kJ · mol⁻¹, $n = 2.3$, and $\log A_D = -3.5$;
- mantle rocks—flow law of dry olivine, with $E = 532$ kJ · mol⁻¹, $n = 3.5$, and $\log A_D = 4.4$.

For porous or fractured media containing a fluid phase, brittle strength is controlled by pore fluid pressure. For the upper crust, a hydrostatic pore fluid pressure gradient with a pore pressure coefficient $\lambda = 0.4$ is generally accepted (e.g., Sibson, 1990). Hydrocarbon exploration wells have shown that in sedimentary basins the transition from a hydrostatic to a near-lithostatic pore pressure gradient generally occurs at a depth of about 3–5 km (e.g., Sibson, 1990). In contrast, the German Continental Deep Drilling Program drill hole has shown that in metamorphic basement rocks a hydrostatic pore-pressure gradient can reach down to at least a 9 km depth and a temperature of 265°C (Huenges et al., 1997; Grawinkel and Stöckert, 1997). For simplicity, in the present simulation we assume a continuous transition from a hydrostatic pore fluid pressure ($\lambda = 0.4$) at the surface to a lithostatic pore fluid pressure ($\lambda = 0.9$) in crustal rocks at a depth of 10 km. Intermediate pore fluid pressures are thus assumed at shallow depths <10 km, with an effective pore-fluid pressure calculated as follows (Gerya et al., 2002b):

$$\lambda = [0.4(10000 - \Delta z_{\text{es}}) + 0.9\Delta z_{\text{es}}]/10000, \quad (12)$$

where Δz_{es} is the depth in m under the calculated dynamic erosion/sedimentation surface. The brittle strength of the mantle is assumed to be high because of the absence of a free pore fluid ($\lambda = 0$ in Equation 8).

As lower and upper bounds for the viscosity of all types of rocks in our numerical experiments, we used 10¹⁶ and 10²⁶ Pa s, respectively.

RESULTS OF NUMERICAL EXPERIMENTS

Figures 8–13 show the results of modeling of the late-orogenic evolution for seven different models of the double-stacked continental crust composed of rocks of granodioritic and dioritic (Figs. 8–10, 12, and 13) or granodioritic and gabbroic (Fig. 11) compositions. As follows from our numerical experiments, this evolution can be subdivided into three stages subsequent to stacking:

1. Thermal relaxation of the stacked continental crust after collision, associated with an increase in density contrast and a decrease in viscosity within the crust, due to an increase in temperature and associated prograde metamorphic reactions (Figs. 8, 11 [0–10 m.y.]; see also Fig 6).

2. Multi-wavelength doming and diapirism in the lower crust, associated with buoyant escape of buried upper continental crust, owing to a low density region and low viscosity flow focused by erosion (Figs. 8, 11, [10–30 m.y.]).

3. Intense regional doming and diapirism in the form of thermal-chemical crustal convection driven by metamorphic phase transformations and associated with gradual ductile rebound of

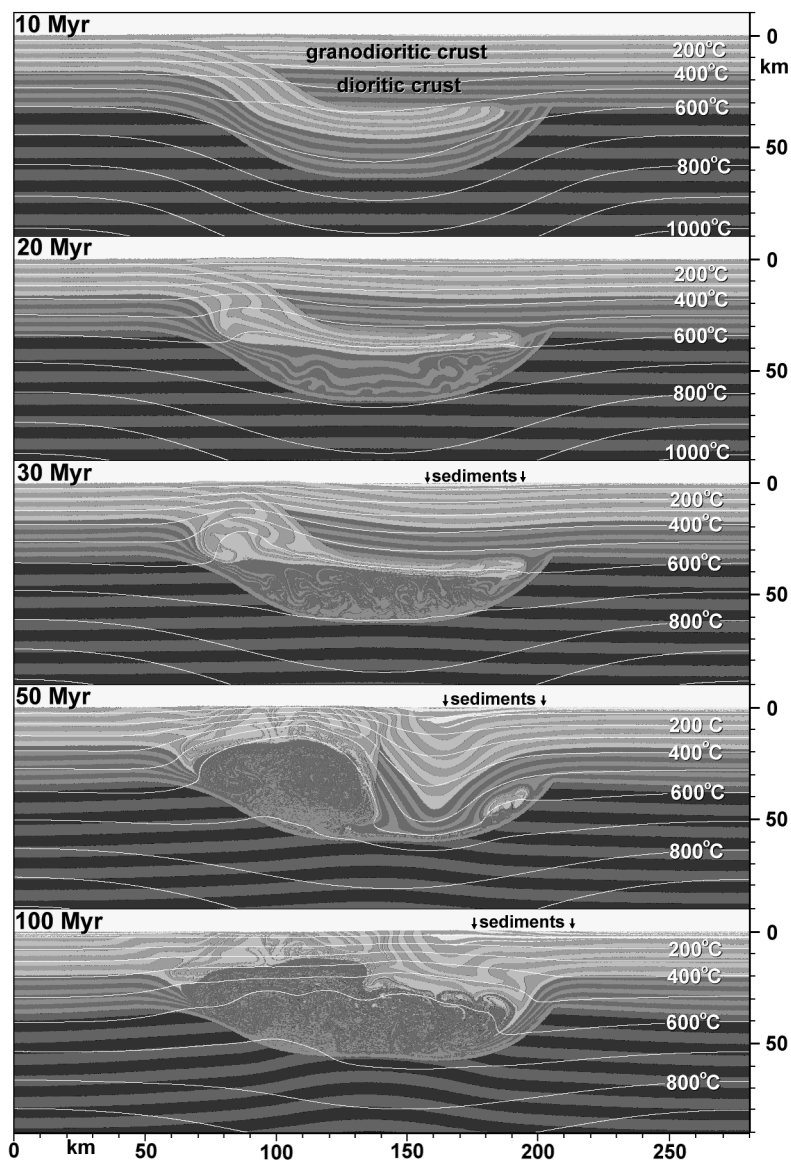


Figure 8. Results of numerical modeling showing the development of doming and diapirism in the double-stacked crust of granodioritic/dioritic composition. White lines represent geotherms in °C. Gray-scale code (color code in electronic version; see the CD-ROM accompanying this volume) as in Figure 7A.

the orogenic root due to the thermal relaxation of the lithospheric mantle under the orogen (Fig. 8, 11 [30–100 m.y.]).

In contrast to the results presented by Arnold et al. (2001), our numerical experiments show a variety of domal and diapiric features. These are related to the heterogeneous multilayered lithological structure of our model, enhanced (Fig. 10) by the influence of prograde phase transformations (e.g., Figs. 1 and 2) proceeding during the thermal relaxation of the crust and following melt-free high temperature metamorphism at lowered water activity (see Equation 1). Another process strongly contributing to the model development is the focusing of exhumation flow (Fig. 9 [30 m.y.]) by brittle weakening of the upper crustal rocks and strain localization by erosion (Ellis et al., 2001). The thickness of the brittle crust depends on the geotherm, strain rate, and

effective rheology. In our experiments, this thickness varies from 10 to 15 km (see the high viscosity layer in the upper part of the model in Fig. 9). The styles of deformation for the brittle and ductile portions of the crust are clearly different (i.e., [1] crustal convection within the ductile region and [2] localized extensional doming; see Tirel et al., this volume) within the brittle crust (Fig. 9 [30 m.y.]). For all studied models, intense doming and diapirism in the form of crustal thermal-chemical convection occur when the temperature at the bottom of the thickened crust reaches ~700 °C, corresponding to the transition between high-grade amphibolite and granulite facies of regional metamorphism (see Fig. 6A).

Figure 12 shows the results of modeling of metamorphic P - T paths for crustal rocks exhumed across a regional dome

structure at 80 m.y. The initial position of the rocks is shown in Figure 12C. A characteristic assemblage of P - T paths corresponds to non-isothermal, non-isobaric metamorphic zoning, resulting from both significant horizontal and vertical displacement (compare Figs. 12B and C) of rocks in an evolving thermal field during gravitational redistribution processes.

Figure 13 shows the influence of changing different physical parameters on the dynamics of doming and diapirism in the double-stacked crust of granodioritic/dioritic composition. The effective rheology of brittle and ductile crust significantly affects gravitational redistribution: Strong, brittle crust precludes focusing of exhumation flow and penetration of high grade rocks toward shallow crustal levels (Fig. 13A), whereas

strong, ductile crust decreases gravitational redistribution rates, preserving the internal geometry of the crust after thermal relaxation (Fig. 13B). In the absence of erosion/sedimentation processes, the focusing of exhumation flow is less efficient, even in combination with a relatively weak brittle rheology of the crust (Fig. 13C). Gravitational redistribution in the form of crustal convection enhanced by phase transformations is efficient, both with and without medium-scale lithological heterogeneity within the crust (cf. Fig. 8 [30 m.y.] and Fig. 13D). However, in the latter case, the convection pattern is more regular and is not complicated by the multi-wavelength diapirism (Fig. 13D) related to the density contrast ($\sim 50 \text{ kg/m}^3$) for medium-scale layering (cf. Fig. 8 [30 m.y.] and Fig. 13E).

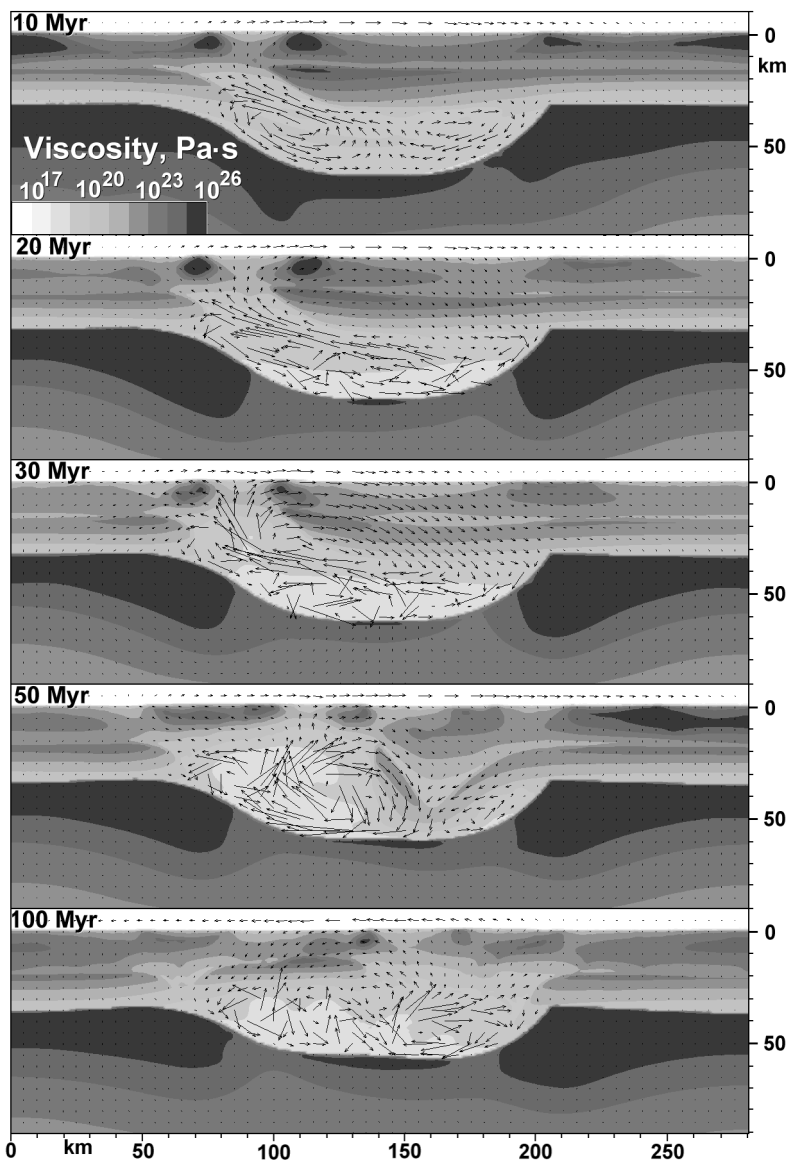


Figure 9. Development of the viscosity structure (gray-scale code here or color code in electronic version; see color version on the CD-ROM accompanying this volume) and velocity field (arrows) for the numerical model shown in Figure 8. Brittle upper portion of the crust is limited to 10–15 km depth and characterized by “Mohr-Coulomb viscosity” varying between 10^{20} and 10^{26} Pa s. Effective creep viscosity of ductile lower portion of the crust varies between 10^{18} and 10^{26} Pa s. Viscosity of the weak layer atop the model is 10^{16} Pa s.

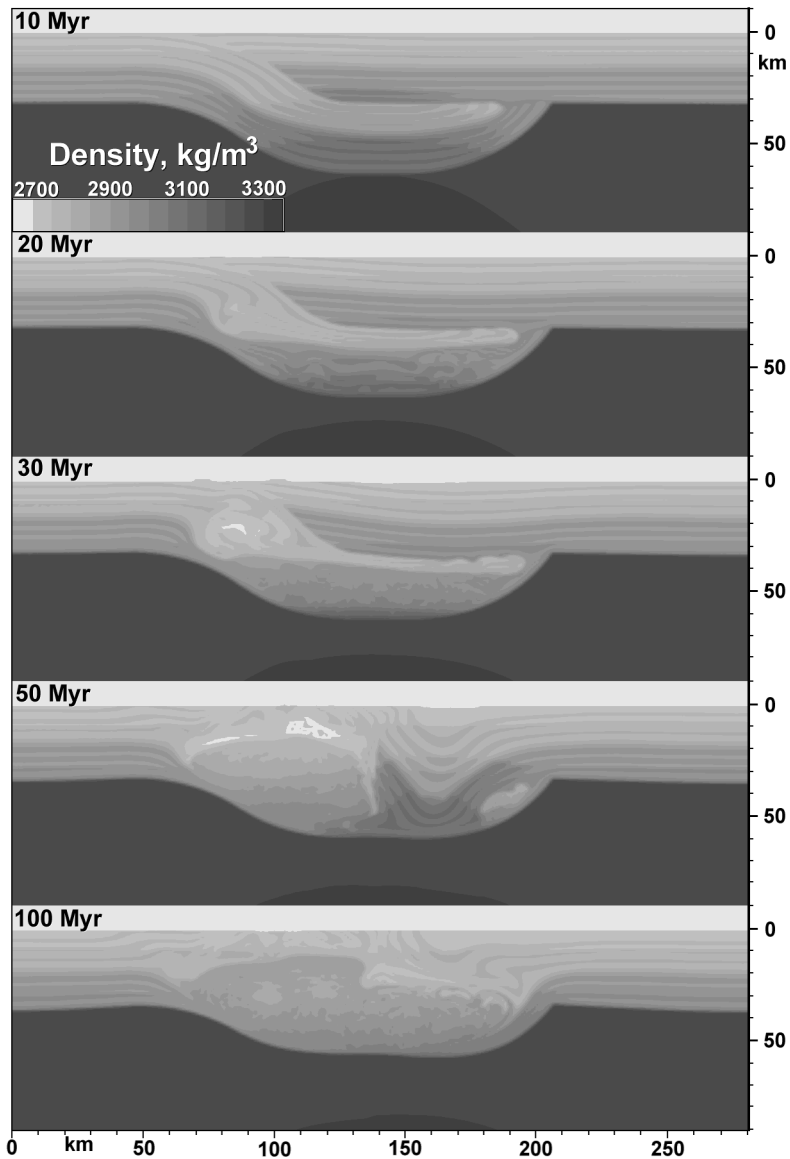


Figure 10. Development of the density structure associated with metamorphic phase transformations in the continental crust for the numerical model shown in Figure 8. A color version of this figure is on the CD-ROM accompanying this volume.

DISCUSSION AND POSSIBLE GEOLOGICAL EXAMPLES

As follows from Figure 3, the decrease in density of major rock types with depth should be a rather common feature in the crust with low- to medium-pressure, high-temperature metamorphism. However, the actual formation of gravitationally unstable density profiles within continental crust will also depend on the evolution of the geothermal gradient, on changes in chemical composition of the crust with depth, and on the kinetics of metamorphic phase transformations (especially in the upper low-grade portion of the crust, in which a high density layer can form). Furthermore, possible gravitational redistribution will depend on the evolution of the degree of gravitational instability and the effective rheology of the crust during and after high-grade

metamorphism. It can be argued that the gravitational instability of the crust related to metamorphic phase transformations may in many respects be similar to the instability induced by partial melting of the crust (e.g., Bittner and Schmeling, 1995). For high-grade metamorphic complexes, both sources of instability should be considered as important factors that may crucially affect the dynamics of exhumation of high-grade rocks.

The strong correlation between the degree of lithological gravitational instability and the calculated steady-state temperature within the lower part of the continental crust suggests that a gravitationally unstable crust will logically lead to further modifications, with a positive feedback effect on gravitational redistribution. Higher geotherms will trigger prograde changes in mineral assemblages, leading to a further enhancement of vertical density inversions (Fig. 6C; see also Gerya et al., 2001),

or, given suitable water fugacities, to the generation of granitic magmas and low-viscosity, partially molten zones in the lower part of the stacked crust (e.g., Arnold et al., 2001). Gravitational redistribution should not only lead to a decrease in gravitational energy, and, as a result, to a more stable structure of the crust, but should also favor a final structure in which abundant mafic, low-heat-productivity and high-density rocks should predominate in the lower part of this crust (Fig. 8, 11).

On the basis of our calculations, it can be concluded that the existence of either relatively homogeneous or heterogeneous multilayered hot continental crust creates very favorable conditions for the onset of the processes of doming and diapirism. The initiation of gravitational redistribution is triggered by a decrease in effective rock viscosities and an enhancement of the gravitational instability by metamorphic phase transformations

during the heating of the crust. Apart from multiscale doming and diapirism, gravitational redistribution processes in the thickened continental crust created by collision may also include buoyant escape or extrusion (“squeezing”) of lower density upper crustal slices buried by regional stacking (Figs. 8, 9, and 11 [10–30 m.y.]). This particular process has also been suggested to be an important feature at lower temperatures during collision and associated normal faulting (e.g., Chemenda et al., 1995). In the hot continental crust, however, the escape is accommodated by significant penetrative ductile deformation of exhuming units that is different from brittle faulting processes at lower temperatures and/or higher strain rates (e.g., Ranalli, 1995; also see Equation 9).

As noted above, gravitationally unstable crust may be produced in any large-scale process leading to inverted rock-density

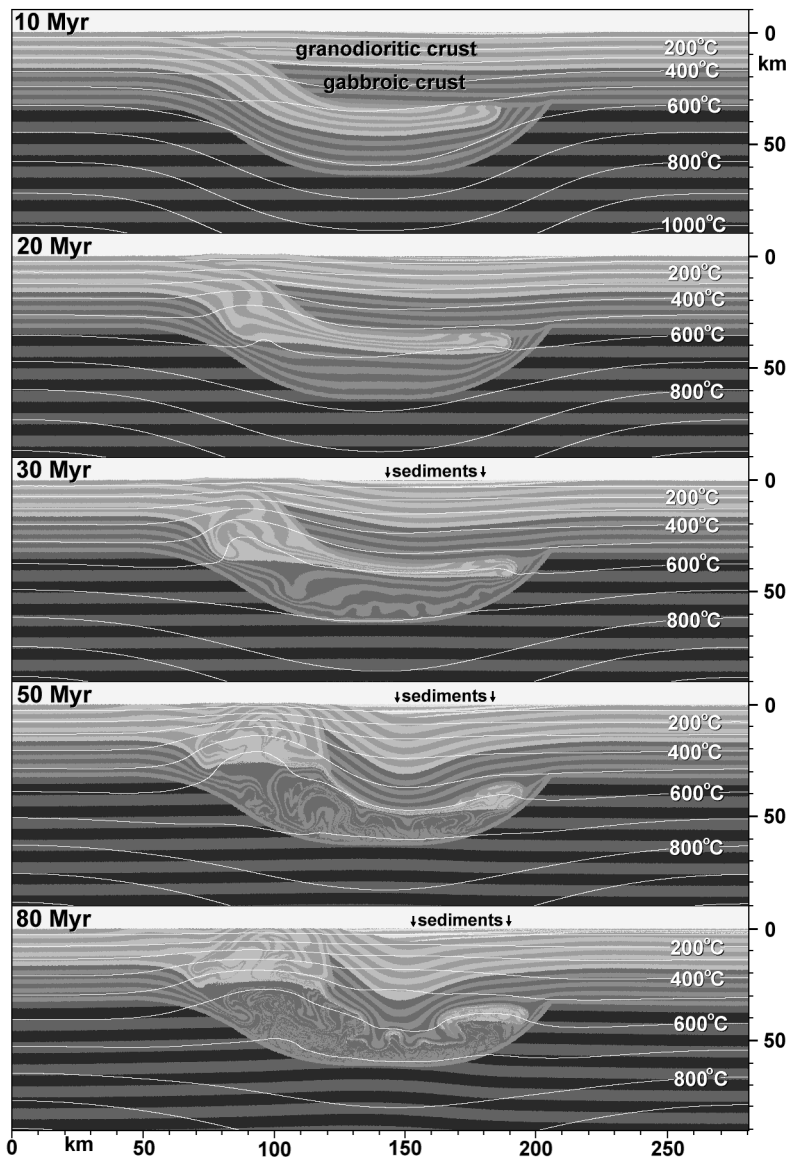


Figure 11. Results of numerical modeling showing the development of doming and diapirism in the double stacked crust of granodioritic/gabbroic composition. White lines represent geotherms in °C. Gray-scale code (color code in electronic version; see the CD-ROM accompanying this volume) as in Figure 7A.

stratifications. Redistribution processes in such crust may have played a significant role in the heat distribution during the formation of Precambrian granite-greenstone terrains (e.g., MacGregor, 1951; Ramberg, 1981) and spatially related granulite complexes (e.g., Perchuk, 1989, 1991; Perchuk et al., 1992, 1999, 2000a, 2000b), where the instability was produced by abundant mafic and ultramafic rocks of greenstone belts overlying sialic basement. However, gravitationally unstable crust is expected to result, above all, from collisional events involving initially stable sections of continental crust, where regional thrusting, multiple stacking, and regional folding occur (e.g., the double-stacked crust of England and Thompson, 1984; Le Pichon et al., 1997). This suggests a strong causal and temporal link between exter-

nal collisional and internal gravitational mechanisms of rock deformation in high-grade metamorphic regions. Collisional mechanisms should operate during the early prograde stages of a tectono-metamorphic cycle, causing thickening of the crust and a corresponding increase in radiogenic thermal supply, whereas gravitational mechanisms should dominate during the later thermal peak and retrograde stages, providing an important factor for regional doming and diapirism (Fig. 8 and 11) contributing to the exhumation (Fig. 12) of high-grade rocks.

A mechanism of buoyant exhumation of granulites driven by the *lithological difference* between upper and lower crustal rocks has already been suggested for several medium-pressure Precambrian granulite complexes (i.e., the Limpopo granulite

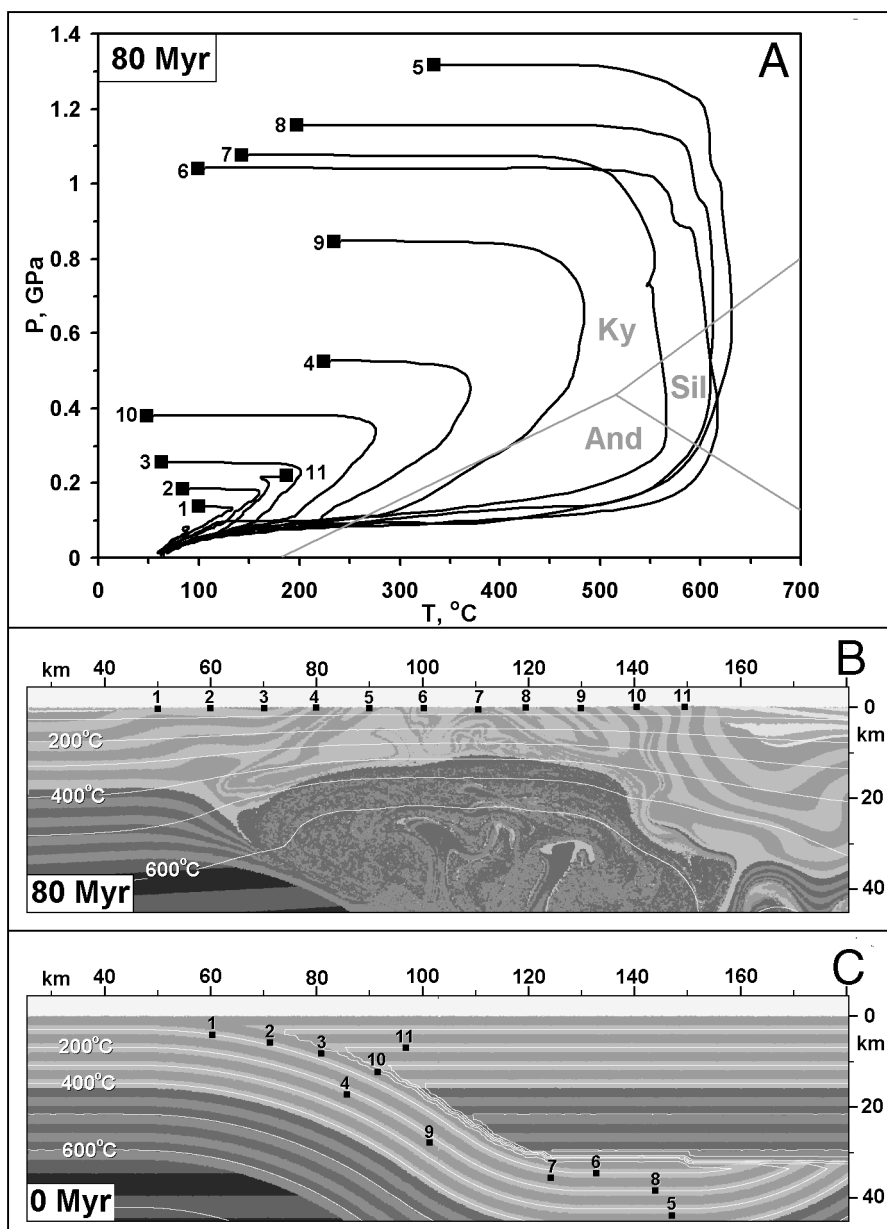


Figure 12. Results of numerical modeling of *P-T* paths for crustal rocks exhumed across the regional domal structure (B) after 80 m.y. 155 × 50 km details of original 280 × 100 km numerical model for crust of granodioritic/dioritic composition (Figs. 7 and 8) are shown in B and C. Numbered solid rectangles in B and C represent final (B) and initial (C) positions of 11 crustal rocks for which the *P-T* paths (A) have been modeled. White lines in B and C represent geotherms in °C. Gray-scale code (color code in electronic version; see the CD-ROM accompanying this volume) as in Figure 7A. A. An assemblage of *P-T* paths obtained across the dome structure; kyanite (Ky), sillimanite (Sil), and andalusite (And) stability fields are shown for orientation. B. Internal geometry of the dome structure and final position of exhumed rocks. C. Initial positions of rocks in double-stacked crust.

complex in South Africa; Perchuk et al., 2000a, 2000b), the Lapland complex in the Kola Peninsula (Perchuk et al., 1999), the Sharizhlagay complex in the Baikal area, Eastern Siberia (Perchuk, 1989), and the Kanskiy granulite complex in the Yenisey Range, Eastern Siberia (Smit et al., 2000). Considering the relatively felsic bulk composition of these complexes (e.g., KG in Table 1), *metamorphic phase transformations* should be considered to be an additional factor, thus increasing the degree of gravitational instability of the crust during high-temperature, medium-pressure metamorphism.

Regional doming related to an extensive low-pressure granulite terrain characterized by an extremely low dP/dT gradient (compare geotherm G in Fig. 1A) is discussed for the Namaqua Mobile Belt of the Northern Cape Province of South Africa (e.g., Gerya et al., 2001). This granulite terrain of the Bushmanland

Subprovince is exposed as a long-wavelength, E-W-trending, dome-like structure of 150–180 km width, gradually passing into upper-amphibolite-facies rocks that overlie the granulites (Waters, 1989; Willner, 1995). At and after the peak of metamorphism, the Namaqua granulites were at a depth level of 12–15 km, where the density of the dominant felsic quartz-bearing rocks under this extreme geothermal gradient must have been considerably less than that of the upper crust (Figs. 1B, 3A). Considering the very long period of cooling, the generally slow, buoyant uprise of the high-grade rocks by about 4 km relative to the amphibolite facies terrain is suggested to have produced the exposed metamorphic zonation (e.g. Gerya et al., 2001).

Another possible example of widespread granulite diapirism can be found in the Bohemian Massif of the Central European Variscan belt. Dome structures that formed late during the

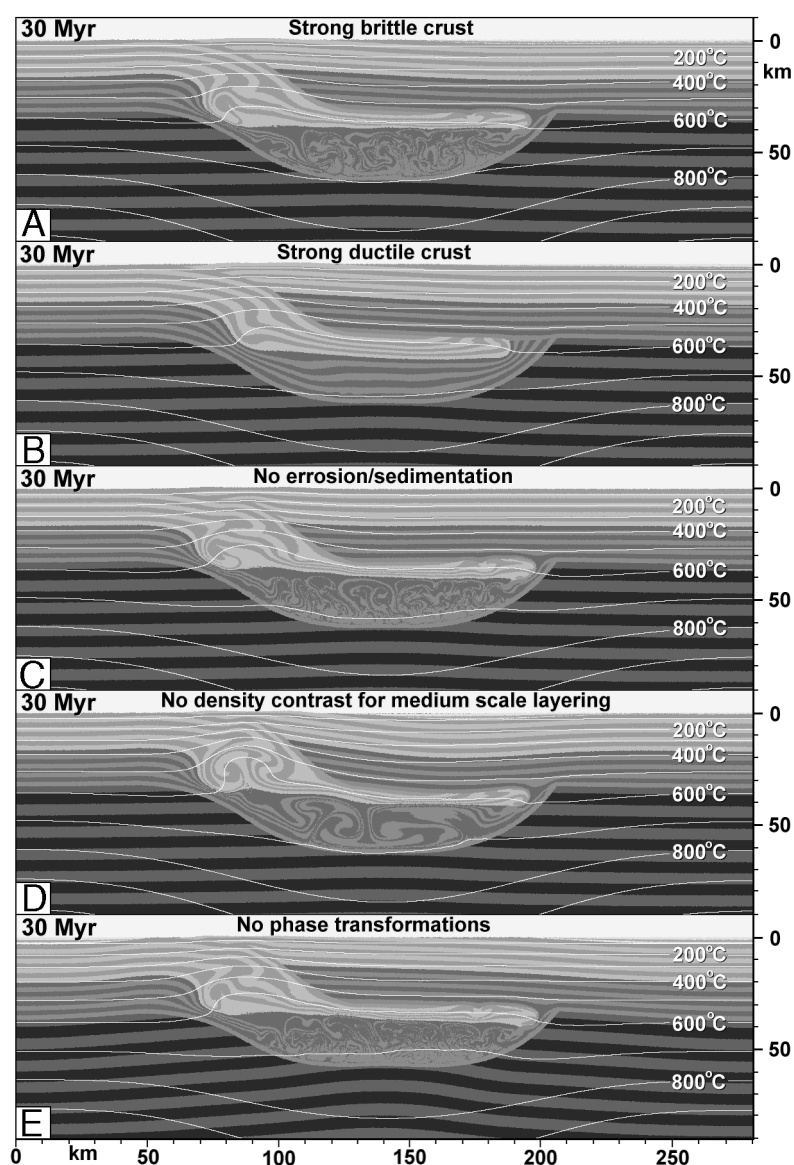


Figure 13. Influence of changes in model parameters on doming and diapirism in the double-stacked crust of granodioritic/dioritic composition (cf. Fig. 8 [30 m.y.]). White lines represent geotherms in °C. A. Strong brittle rheology of the crust ($\lambda = 0.6$ in Equation 9). B. Strong ductile rheology of the crust (implemented by decreasing A_d value in Equation 11 by factor of 10). C. No erosion/sedimentation considered ($v_s = 0$ and $v_e = 0$ in Equation 3). D. No density contrast for medium-scale layering considered (non-compositional layering in the homogeneous upper and lower crust is used to show material displacement). E. No phase transformations considered (density of the granodioritic and dioritic crust is calculated according to Equation 8 using parameters from Table 2; medium-scale layering with a constant 50 kg/m^3 standard density contrast is also used for the crust). Other model parameters and gray-scale as in Figure 8. A color version of this figure is on the CD-ROM accompanying this volume.

orogenic evolution are ubiquitous in this area, concomitant with a late regional high temperature/low pressure metamorphic overprint. As shown by Vrána and Sramek (1999), several isometric dome structures, with diameters of 5–39 km, containing predominantly acidic granulites are characterized by a density of 2620–2660 kg/m³, which is notably lower compared to the surrounding gneissic rocks (2680–2720 kg/m³) and results in a significant negative gravity anomaly.

The most significant negative gravity anomaly of Central Europe is related to the Erzgebirge dome at the northern edge of the Bohemian Massif (Giese, 1995). This area is characterized by several late subdome structures, late granitic intrusions, and a substantial late increase of the geotherm after rapid exhumation of predominantly acidic high temperature–high pressure granulites (Willner et al., 2000). The structurally lowermost subdome (Freiberg dome) shows divergent, ductile, and penetrative extensional deformation of a shallow crustal level, while structurally higher subdomes are characterized by mere buckling without related mesoscopic structures.

Because of the enhancement of the lithological density contrast at high temperatures of granulite metamorphism (e.g., Fig. 6), buoyant uprise of hot granulitic bodies from deeper crustal levels and their implantation into colder gneissic complexes within the middle or upper crust could be a realistic cause for the formation of such late orogenic dome structures.

CONCLUSION

Metamorphic phase transformations proceeding with increasing temperature should be considered as a possible source of gravitational instability, doming, and diapirism in the hot continental crust when low dP/dT geotherms are characteristic. Thus, regional high-temperature amphibolite and granulite facies metamorphism might be “genetically” related to an increase in the degree of gravitational instability within either relatively *homogeneous* or *heterogeneous* multilayered sections of the continental crust. Metamorphic phase transformations, partial melting, and thermal expansion of minerals can be expected to accompany exponential lowering of the effective viscosity of rocks with increasing temperature. This can lead to the activation of crustal doming and diapirism that in turn result in significant displacement and complex deformation (e.g., Figs. 8 and 11) of metamorphic rocks within the hot continental crust (e.g., Belousov, 1989; Perchuk, 1989, 1991; Perchuk et al., 1992, 1999, 2000a, 2000b; Weinberg and Schmeling, 1992; Dirks, 1995; Bittner and Schmeling, 1995; Gerya et al., 2000, 2001, 2002a; Arnold et al., 2001).

ACKNOWLEDGMENTS

This work was supported by Russian Foundation of Basic Research grants 02-05-64025, 03-05-64633, and 1645-2003-5, by Swiss Federal Institute of Technology research Grant TH-12/04-1, and by an Alexander von Humboldt Foundation Research Fellowship to T.V. Gerya, and by the Sonderforschungsbereich

526 at Ruhr-University, funded by the Deutsche Forschungsgemeinschaft. Constructive reviews by S. Ellis and an anonymous reviewer are greatly appreciated.

REFERENCES CITED

- Arnold, J., Jacoby, W.R., Schmeling, H., and Schott, B., 2001, Continental collision and the dynamic and thermal evolution of the Variscan orogenic crustal root—numerical models: *Journal of Geodynamics*, v. 31, p. 273–291, doi: 10.1016/S0264-3707(00)00023-5.
- Belousov, V.V., 1989, *Geotectonics*: Moscow, Nedra Press, 381 p. (in Russian).
- Bittner, D., and Schmeling, H., 1995, Numerical modeling of melting processes and induced diapirism in the lower crust: *Geophysical Journal International*, v. 123, p. 59–70.
- Brace, W.F., and Kohlstedt, D.L., 1980, Limits on lithospheric stress imposed by laboratory experiments: *Journal of Geophysical Research*, v. 85, p. 6248–6252.
- Chemenda, A.I., Mattauer, M., Malavieille, J., and Bokun, A.N., 1995, A mechanism for syn-collisional deep rock exhumation and associated normal faulting: Results from physical modeling: *Earth and Planetary Science Letters*, v. 132, p. 225–232, doi: 10.1016/0012-821X(95)00042-B.
- Clauser, C., and Huenges, E., 1995, Thermal conductivity of rocks and minerals, in Ahrens, T.J., ed., *Rock Physics and Phase Relations*, AGU Reference Shelf 3: Washington, D.C., AGU, p. 105–126.
- Conrad, C.P., and Molnar, P., 1997, The growth of Rayleigh-Taylor-type instabilities in the lithosphere for various rheological and density structures: *Geophysical Journal International*, v. 129, p. 95–112.
- Conrad, C.P., and Molnar, P., 1999, Convective instability of a boundary layer with temperature- and strain-rate-dependent viscosity in term of ‘available buoyancy’: *Geophysical Journal International*, v. 139, p. 51–68, doi: 10.1046/J.1365-246X.1999.00896.X.
- Dale, J., Holland, T.J.B., and Powell, R., 2000, Hornblende-garnet-plagioclase thermobarometry: A natural assemblage calibration of the thermodynamics of hornblende: *Contributions to Mineralogy and Petrology*, v. 140, p. 353–362, doi: 10.1007/S004100000187.
- de Capitani, C., and Brown, T.H., 1987, The computation of chemical equilibrium in complex systems containing non-ideal solid solutions: *Geochimica et Cosmochimica Acta*, v. 51, p. 2639–2652, doi: 10.1016/0016-7037(87)90145-1.
- De Wit, M.J., and Ashwal, L.D., 1997, *Greenstone Belts*: Oxford, Clarendon Press, 809 p.
- Dirks, P.H.G.M., 1995, Crustal convection: Evidence from granulite terrains: *Centennial Geocongress, Extended Abstracts, The Geological Society of Southern Africa*, v. 2, p. 673–676.
- Ellis, S., Wissing, S., Beaumont, C., and Pfiffner, A., 2001, Strain localisation as a key to reconciling experimentally derived flow-law data with dynamic models of continental collision: *International Journal of Earth Sciences*, v. 90, p. 168–180, doi: 10.1007/S005310000151.
- England, P.C., and Thompson, A.B., 1984, Pressure-temperature-time paths of regional metamorphism; I, Heat transfer during the evolution of regions of thickened continental crust: *Journal of Petrology*, v. 25, p. 894–928.
- Gerya, T.V., Perchuk, L.L., van Reenen, D.D., and Smit, C.A., 2000, Two-dimensional numerical modeling of pressure-temperature-time paths for the exhumation of some granulite facies terrains in the Precambrian: *Journal of Geodynamics*, v. 30, p. 17–35, doi: 10.1016/S0264-3707(99)00025-3.
- Gerya, T.V., Maresch, W.V., Willner, A.P., Van Reenen, D.D., and Smit, C.A., 2001, Inherent gravitational instability of thickened continental crust with regionally developed low- to medium-pressure granulite facies metamorphism: *Earth and Planetary Science Letters*, v. 190, p. 221–235, doi: 10.1016/S0012-821X(01)00394-6.
- Gerya, T.V., Perchuk, L.L., Maresch, W.V., Willner, A.P., Van Reenen, D.D., and Smit, C.A., 2002a, Thermal regime and gravitational instability of multi-layered continental crust: implications for the buoyant exhumation of high-grade metamorphic rocks: *European Journal of Mineralogy*, v. 14, p. 687–699, doi: 10.1127/0935-1221/2002/0014-0687.
- Gerya, T.V., Stöckhert, B., and Perchuk, A.L., 2002b, Exhumation of high-pressure metamorphic rocks in a subduction channel: A numerical simulation: *Tectonics*, v. 21, p. 6–16–19, doi: 10.1029/2002TC001406.
- Giese, P., 1995, Main features of geophysical structures in Central Europe, in Dallmeyer, R.D., Franke, W., and Weber, K., eds., *Pre-Permian geology of Central and Eastern Europe*: Berlin, Springer-Verlag, p. 7–25.

- Grawinkel, A., and Stöckhert, B., 1997, Hydrostatic pore fluid pressure to 9 km depth—Fluid inclusion evidence from the KTB deep drill hole: *Geophysical Research Letters*, v. 24, p. 3273–3276, doi: 10.1029/97GL03309.
- Gurnis, M., Eloy, C., and Zhong, S., 1996, Free-surface formulation of mantle convection—II. Implication for subduction-zone observables: *Geophysical Journal International*, v. 127, p. 719–727.
- Harley, S.L., 1989, The origin of granulites: A metamorphic perspective: *Geological Magazine*, v. 126, p. 215–231.
- Holland, T.J.B., and Powell, R., 1998, Internally consistent thermodynamic data set for phases of petrological interest: *Journal of Metamorphic Geology*, v. 16, p. 309–344.
- Holland, T.J.B., Baker, J., and Powell, R., 1998, Mixing properties and activity-composition relationships of chlorites in the system $\text{MgO-FeO-Al}_2\text{O}_3\text{-SiO}_2\text{-H}_2\text{O}$: *European Journal of Mineralogy*, v. 10, p. 395–406.
- Houseman, G., and Molnar, P., 1997, Gravitational (Rayleigh-Taylor) instability of a layer with non-linear viscosity and convective thinning of continental lithosphere: *Geophysical Journal International*, v. 128, p. 125–150.
- Huenges, E., Erzinger, J., Kuck, J., Engeser, B., and Kessels, W., 1997, The permeable crust: Geohydraulic properties down to 9101 m depth: *Journal of Geophysical Research*, v. 102, p. 18255–18265, doi: 10.1029/96JB03442.
- Johannes, W., 1985, The significance of experimental studies for the formation of migmatites, in Ashworth, J.A., ed., *Migmatites*: Glasgow, Blackie, p. 36–85.
- Jull, M., and Kelemen, P.B., 2001, On the conditions for lower crustal convective instability: *Journal of Geophysical Research*, v. 106, p. 6423–6446, doi: 10.1029/2000JB900357.
- Karpov, I.K., Kiselev, A.I., and Letnikov, F.A., 1976, Computer modeling of natural mineral formation: Moscow, Nedra Press, 256 p. (in Russian).
- Kretz, R., 1983, Symbols for rock-forming minerals: *American Mineralogist*, v. 68, p. 277–279.
- Krohe, A., 1998, Extending a thickened crustal bulge: toward a new geodynamic evolution model of the Paleozoic NW Bohemian Massif, German Continental Deep Drilling site (SE Germany): *Earth-Science Reviews*, v. 44, p. 95–145, doi: 10.1016/S0012-8252(98)00028-2.
- Le Pichon, X., Henry, P., and Goffe, B., 1997, Uplift of Tibet: from eclogites to granulites—implications for the Andean Plateau and the Variscan belt: *Tectonophysics*, v. 273, p. 57–76, doi: 10.1016/S0040-1951(96)00288-0.
- MacGregor, A.M., 1951, Some milestones in the Precambrian of Southern Rhodesia: *Transactions of the Geological Society of South Africa*, v. 54, p. 27–71.
- McLennan, S., 1992, Continental crust: *Encyclopedia of Earth Science*, v. 1, p. 1085–1098.
- Molnar, P., Houseman, G., and Conrad, C., 1998, Rayleigh-Taylor instability and convective thinning of mechanically thickened lithosphere: Effects of non-linear viscosity decreasing exponentially with depth and of horizontal shortening of the layer: *Geophysical Journal International*, v. 133, p. 568–584, doi: 10.1046/j.1365-246x.1998.00510.x.
- Nozkhin, A.D., and Turkina, O.M., 1993, Geochemistry of granulites: Reports of Institute of Geology and Geophysics Russian Academy of Sciences, Novosibirsk, v. 817, p. 224.
- Perchuk, L.L., 1989, P-T-fluid regimes of metamorphism and related magmatism with specific reference to the Baikal Lake granulites, in Daly, S., Yardley, B.W.D., and Cliff, B., eds., *Evolution of Metamorphic Belts*: London, Geological Society Special Publication 42, p. 275–291.
- Perchuk, L.L., 1991, Studies in magmatism, metamorphism and geodynamics: *International Geology Review*, v. 33, p. 311–374.
- Perchuk, L.L., Podladchikov, Y.Y., and Polaykov, A.N., 1992, P-T paths and geodynamic modelling some metamorphic processes: *Journal of Metamorphic Geology*, v. 10, p. 311–319.
- Perchuk, L.L., Krotov, A.V., and Gerya, T.V., 1999, Petrology of amphibolites of the Tanaelv Belt and granulites of the Lapland complex: *Petrology*, v. 7, p. 539–563.
- Perchuk, L.L., Gerya, T.V., Van Reenen, D.D., Krotov, A.V., Safonov, O.G., Smit, C.A., and Shur, M.Y., 2000a, Comparable petrology and metamorphic evolution of the Limpopo (South Africa) and Lapland (Fennoscandia) high-grade terrains: *Mineralogy and Petrology*, v. 69, p. 69–107, doi: 10.1007/S007100050019.
- Perchuk, L.L., Gerya, T.V., Van Reenen, D.D., Smit, C.A., and Krotov, A.V., 2000b, P-T paths and tectonic evolution of shear zones separating high-grade terrains from cratons: examples from Kola Peninsula (Russia) and Limpopo region (South Africa): *Mineralogy and Petrology*, v. 69, p. 109–142, doi: 10.1007/S007100050020.
- Poliakov, A.N.B., and Podladchikov, Y., 1992, Diapirism and topography: *Geophysical Journal International*, v. 109, p. 553–564.
- Poliakov, A.N.B., van Balen, R., Podladchikov, Yu., Daudre, B., Cloetingh, S., and Talbot, C., 1993, Numerical analysis of how sedimentation and redistribution of surficial sediments affects salt diapirism: *Tectonophysics*, v. 226, p. 199–216, doi: 10.1016/0040-1951(93)90118-4.
- Powell, R., and Holland, T.J.B., 1999, Relating formulations of the thermodynamics of mineral solid solutions: Activity modeling of pyroxenes, amphiboles, and micas: *American Mineralogist*, v. 84, p. 1–14.
- Ramberg, H., 1981, *Gravity, deformation and geological application*: London, Academic Press, 452 p.
- Ranalli, G., 1995, *Rheology of the Earth*, 2nd ed.: London, Chapman and Hall, 413 p.
- Rudnick, R.L., and Fountain, D.M., 1995, Nature and composition of the continental crust: A lower crustal perspective: *Reviews of Geophysics*, v. 33, p. 267–309, doi: 10.1029/95RG01302.
- Schott, B., and Schmeling, H., 1998, Delamination and detachment of a lithospheric root: *Tectonophysics*, v. 296, p. 225–247, doi: 10.1016/S0040-1951(98)00154-1.
- Sibson, R.H., 1990, Faulting and fluid flow, in Nesbitt, B.E., ed., *Fluids in tectonically active regimes of the continental crust*: Vancouver, Mineralogical Association of Canada, p. 92–132.
- Smit, C.A., Van Reenen, D.D., Gerya, T.V., Varlamov, D.A., and Fed'kin, A.V., 2000, Structural-metamorphic evolution of the Southern Yenisey Range of Eastern Siberia: Implications for the emplacement of the Kanskiy granulite Complex: *Mineralogy and Petrology*, v. 69, p. 35–67, doi: 10.1007/S007100050018.
- Sobolev, S.V., and Babeyko, A.Yu., 1994, Modeling of mineralogical composition, density and elastic wave velocities in anhydrous magmatic rocks: *Surveys in Geophysics*, v. 15, p. 515–544.
- Spear, F.S., 1993, *Metamorphic phase equilibria and pressure-temperature-time paths*: Washington, D.C., Mineralogical Society of America Monograph, 799 p.
- Thompson, A.B., 1990, Heat, fluids, and melting in the granulite facies, in Vielzeuf, D., and Vidal, Ph., eds., *Granulites and Crustal Evolution*: NATO ASI Series, Series C, Kluwer (Dordrecht), v. 311, p. 37–58.
- Turcotte, D.L., and Schubert, G., 1973, Frictional heating of the descending lithosphere: *Journal of Geophysical Research*, v. 78, p. 5876–5886.
- Turcotte, D.L., and Schubert, G., 1982, *Geodynamics: Applications of continuum physics to geological problems*: New York, John Wiley, 450 p.
- Vrána, S., and Sramek, J., 1999, Geological interpretation of detailed gravity structure of the granulite complex in southern Bohemia and its structure: *Vestník Českého Geologického Ústavu*, v. 74, p. 261–278.
- Waters, D.J., 1989, Metamorphic evidence for the heating and cooling path of Namaqualand granulites, in Daly, J.S., Cliff, R.A., and Yardley, B.W.D., eds., *Evolution of Metamorphic Belts*: London, Geological Society Special Publication 40, p. 357–363.
- Weinberg, R.B., and Schmeling, H., 1992, Polydiapirs: Multiwavelength gravity structures: *Journal of Structural Geology*, v. 14, p. 425–436, doi: 10.1016/0191-8141(92)90103-4.
- Willner, A.P., 1995, Pressure-temperature evolution of a low-pressure amphibolite facies terrane in Central Bushmanland (Namaqua Mobile Belt; South Africa): Special Publication: Geological Survey of Namibia, v. 15, p. 5–19.
- Willner, A.P., Krohe, A., and Maresch, W.V., 2000, Interrelated PTtd-paths in the Variscan Erzgebirge Dome (Saxony/Germany): Constraints for the rapid exhumation dynamics of HP-HT rocks from the root zone of a collisional orogen: *International Geology Reviews*, v. 42, p. 64–85.
- Yardley, B.W.D., 1989, *An introduction to metamorphic petrology*: Harlow, UK, Longman, Earth Sciences Series, 248 p.

